Master's thesis

NTNU
Norwegian University of Science and Technology
Faculty of Engineering
Department of Energy and Process Engineering

Torgeir Andersen

Hydrogen and Wet Gas Compressor Analysis

Master's thesis in Mechanical Engineering
Supervisor: Professor Lars Eirik Bakken
June 2020

NTNU
Norwegian University of
Science and Technology

NTNU
Norwegian University of
Science and Technology

Hydrogen and Wet Gas Compressor Analysis

Torgeir Andersen

June 9, 2020

Master in Mechanical Engineering
30 ECTS
Department of Energy and Process Engineering
Norwegian University of Science and Technology

Supervisor: Prof. Lars Eirik Bakken

Co-Supervisor: Tor Bjørge, Equinor

Co-Supervisor: Chief Engineer Erik Langørgen

Contents

List of Figures

List of Tables

Nomenclature

a	sonic velocity	[m/s]
b	impeller tip width	[m]
c	absolute velocity	[m/s]
c_p	isobaric heat capacity	[J/K]
c_θ	tangential velocity	[m/s]
c_v	isochoric heat capacity	[J/K]
D_h	hydraulic diameter	[m]
f	compression path correction factor	[-]
g	gravitational acceleration	[m/s^2]
H	head	[J/kg]
h	enthalpy	[J/kg]
I	polar inertia	[kg/m^2]
K	isentropic exponent	[-]
KE	kinetic energy	[J]
k_s	equivalent sand roughness	[m]
M	molecular weight	[g/mol]
$\dot{m}$	mass flow rate	[kg/s]
N	rotational speed	[min^{-1}]
n	polytropic exponent	[-]
n_T	polytropic temperature exponent	[-]
n_v	polytropic volume exponent	[-]

P	power	[W]
p	pressure	[Pa]
Q	volume flow rate	[m^3/s]
Q_h	heat transfer	[J]
$\dot{Q}$	energy rate, heat	[W]
R_0	general gas constant	[J/kgK]
R_a	technical roughness	[μm]
Re	Reynolds number	[-]
T	temperature	[K]
u	impeller velocity	[m/s]
V	volume	[m^3]
W	work	[J]
$\dot{W}$	energy rate, work	[W]
ΔW	specific work transfer	[J/kgs]
w	relative velocity	[m/s]
Z	compressibility factor	[-]
z	height	[m]
α	angle between c and u	[°]
β	angle between c and w	[°]
η	efficiency	[-]
γ	ratio of specific heats	[-]
λ	friction coefficient	[-]
ω	angular speed	[s^{-1}]
ν	kinematic viscosity	[m^2/s]

Subscripts

01	inlet stagnation
02	outlet stagnation
1	inlet
2	outlet
$2s$	isentropic outlet
a	given operation point
b	calculated operation point
c	compressor
cr	critical
p	polytropic
s	isentropic
sp	set point condition
t	test operating condition
tot	total

Abstract

The energy industry is facing multiple challenges as a result of the world's strive to minimize the carbon footprint. Innovation in low and zero CO_2 emitting energy production and high expectations of further innovation result in the need for a transfer and storage medium for this green energy. Petroleum products such as methane gas, petrol and diesel may not be environmentally friendly, but they are extremely practical. Their high energy density and relatively low production cost have made it possible to for exampel travel farther, faster and cheaper. To phase out petroleum products will not be an easy task, but compressed hydrogen gas is looked upon as a possible replacement. For this to happen large scale, cost effective compression of hydrogen gas has to become a reality. The petroleum industry has for many years driven the innovation of compressing gas. Centrifugal compressors are widely used for compressing natural gas for storage and pipeline transportation. In order to utilize these compressors for hydrogen gas, their behaviour while running on hydrogen must be studied and understood.

During this project compressor performance for the NTNU wet gas compressor test facility has been experimentally established. A conversion procedure has been made, approximating the compressors performance on hydrogen gas based on it's performance on air, showing a significant reduction in pressure ratio for the compressor if it were to compress hydrogen gas.

Driver trip tests with and without tuning of the rundown trajectory were conducted. Ramping down the discharge throttle valve was the technique used to tune the trajectory. A Hysys Dynamics based process model was tuned to the compressor's performance characteristics and trip with and without ramping of the discharge throttle valve was simulated. The results were promising, with high levels of accuracy and the general non-surging behaviour of the compressor during trip was well replicated in the simulations. As for simulations of surge, the model became numerically unstable. Trip simulations with the discharge valve blocking the outlet of the compressor was also conducted, only to confirm that Hysys dynamics is not yet suited for simulations of surge.

The tuned Hysys model was also used to investigate the compressor's behaviour during transient operation while compressing Hydrogen gas. Here Hysys displayed promising results. Additionally, this highlighted the necessity of further investigation as a low impeller breaking effect of hydrogen gas during trip was present which, among several factors, could be important for hydrogen gas compressor operating with a high pressure increase.

Sammendrag

Verdens energiproduserende industri står overfor flere utfordringer i sin søken etter å minimere utslippene av drivhusgasser. Nyvinninger i lav- og nullutslipps energiproduksjon og forventninger om videre innovasjon resulterer i et behov for et transport- og lagringsmedium til denne miljøvennlige energien. Petroleumsprodukter som metangass, bensin og diesel er alt annet enn miljøvennlige, men med sin høye energitetthet og lav kostnad svært anvenlige. Utfasingen av petroleumsprodukter blir ikke en enkel oppgave. Komprimert hydrogengass blir sett på som en mulig erstatning. For å få til dette må storskala, kostnadseffektiv kompresjon av hydrogengass bli en realitet. Petroleumsindustrien har i en årrekke drevet utviklingen av gasskomprimering, og sentrifugalkompressorer er hyppig brukt til å komprimere naturgass for lagring og transport via rørledninger. For å kunne nyttiggjøre kompressorer av denne typen til bruk på hydrogengass må det undersøkes hvordan sentrifugalkompressorer opererer ved komprimering av denne gassen.

I løpet av prosjektet har kompressorkarakteristikken for NTNU sin våtgasskompressor ved komprimering av luft blitt eksperimentelt fastsatt. En konverteringsprosedyre har blitt lagd for å tilnærme kompressorens ytelse ved komprimering av hydrogen basert på kompressorkarateristikken. Denne viste en markant reduksjon i trykkforhold over kompressoren for hydrogengass relativt til luft.

Systemresponsen til kompressoren ved tap av drivkraft ble også undersøkt. Lukking av utløpsventilen ble brukt til å justere nedkjøringsforløpet til kompresoren. En dynamisk modell i prosessimuleringsprogrammet Aspen Hysys ble justert til å gjengi kompresorkarakteristikken til kompressoren. Videre ble simuleringer med tap av drivkraft simulert både med og uten lukking av utløpsventil. Simuleringene var lovende, med en god gjengivelse av systemresponsen til kompressoren. For simuleringer hvor kompressoren opererer i det ustabile området av kompressorkarakteristikken (surge-området) ble modellen numerisk ustabil. Simuleringer med tap av drivkraft og blokkering av kompressorutløpet ble også gjennomført. Disse simuleringene bekreftet Hysys dynamics manglende evne til å simulere kompressorer i surge.

Den justerte Hysysmodellen ble også brukt til å undersøke kompressorens systemrespons ved komprimering av hydrogengass. Her viste Hysys nok en gang lovende resultater. I tillegg fremhevet modellen nødvendigheten av videre undersøkelser da blant annet bremseffekten hydrogengassen har på kompressorens impeller kan være en viktig faktor for hydrogenkompressorer som opererer med et høyere trykkforhold enn angitt i denne oppgaven.

Preface

This Master's thesis was performed during the spring of 2020, and marks the end of my time as a student. Due to the Covid-19 pandemic this work could not be carried out in an ordinary manner. I would like to praise NTNU for acting swiftly regarding the closing of all campuses, and managing a high information flow to the students during this time.

My supervisor, Professor Lars Eirik Bakken, is as deserving of gratitude as a supervisor could be. For being a resource in himself and for having an emphasis on teaching in a manner where students get a deep understanding of turbomachinery, I thank him. A special thanks to lab-engineer Erik Langørgen for his practical know-how and to Martin Bakken for his help with the dynamic Hysys model.

I would also like to thank my parents for letting me take over the living room and use the dining table as my office as this thesis was written in Haugesund due to Covid-19. Additionally I thank them, and my girlfriend, for unconditional support and motivation.

I end off with a quote by Winston Churchill, in a somewhat more optimistic manner than he uttered it in November 1942: "Now this is not the end. It is not even the beginning of the end. But it is, perhaps, the end of the beginning."

Torgeir Andersen
Haugesund, June 2020

1 Introduction

1.1 Background

As a result of the industrial revolution the world has become totally dependent on fossil fuels for generating energy to our cities and our means of transportation. As the awareness around global warming has increased, the search for zero emission alternatives to petroleum and coal has intensified. Wind-, solar-, hydro- and nuclear energy are to be considered as today's most promising candidates to make the world less dependent on fossil fuels. Along with these new sources of energy, problems with transportation and storage of this energy arise. One of the biggest advantages of petroleum is it's high energy density. Most zero emission energy sources generates it's energy in the form of electricity. As of today, storage of electricity is limited as the energy density of batteries can't even come close to that of for example petrol. This results in a need for a medium to transport and store energy in an energy-dense form. Hydrogen has been called out as a strong candidate for the job, where methods for creating high volumetric energy density hydrogen includes cryogenic liquefaction, chemical storage like metal hydrides and compressed hydrogen gas. This project will focus on the latter of these.

As compressor testing facilities are costly, especially when working with flammable gasses like hydrogen, a lot can be gained by creating and using dynamic models like Hysys dynamics is capable of running. These models need to be accurate for compressors operating at stable conditions and during transient operation. The possibility of predicting the performance of a compressor on hydrogen based on it's performance on air could be vital in the development of hydrogen compressors. Such a tool could also in some instances be used to determine whether or not existing compressor designs could be used in hydrogen gas processing.

1.2 Problem description

During the work with this thesis, the problem description had to be changed as a result of time limitations and various unexpected obstacles. Focus was, in consultation with supervisor, shifted to a more general analysis rather than focusing on the extreme 700 bar pressure in the problem description.

The problem description reads as follows:

Hydrogen is one key element to reduce emission and related environmental impact. Applications within aviation and transportation require low temperature and high-pressure to compensate for the low volumetric energy content at standard conditions. High gas pressure, in the range of 700 to 800 bar is favourable but represents a considerable challenge related to the compressor steady state and transient analysis.

An estimate of hydrogen performance may be calculated based on the NTNU wet gas test lab compressor performance at atmospheric air conditions.

The following tasks to be considered:

1. Establish relevant compressor performance characteristics at dry air conditions and establish procedure to transfer dry air performance to hydrogen performance.
2. Test, fine tune and validate the Wet Gas Compressor Hysys model for steady operation and trip.
3. Use the validated Hysys model to simulate the compressor on hydrogen gas during steady operation and trip.

2 Principles of centrifugal compressors

Some of the main principles of centrifugal compressors and their operation are listed in this chapter, with focus on the principles and relations relevant for this thesis.

2.1 Energy equations

In many cases, especially for large scale industrial applications, the compressor is tailor-made. Usually the differences between the different centrifugal compressors are most noticeable by looking at the impeller. The size, amount and geometry of the impeller vanes all affect how it acts on the fluid and change the velocity triangle of the compressor. A velocity triangle is a way of relate the impeller speed, relative (to the impeller) velocity of the fluid and the absolute velocity of the fluid to each other. Usually an impeller is designed with regard to the velocity triangle of the inlet and the outlet of the impeller. The absolute velocity out from the impeller (c_2) is directly linked with the work done to the fluid as Çengel and Boles [1] demonstrated through the first law of thermodynamics with equation 2.1, and applying it to a steady flow of fluid through a control volume resulting in equation 2.2. It is this kinetic energy that is transformed into pressure energy by the diffuser.

$$\oint (dQ_h - dW) = 0 \tag{2.1}$$

$$\dot{Q} - \dot{W} = \dot{m}[(h_2 - h_1) + \frac{1}{2}(c_2^2 - c_1^2) + g(z_2 - z1)] \tag{2.2}$$

For a compressor, the contribution of the potential energy is negligible because of a relatively small Δz. In addition, a compressor is usually assumed to be adiabatic so that $\dot{Q} = 0$, simplifying equation 2.2 to equation 2.3.

$$-\dot{W} = \dot{m}[(h_2 - h_1) + \frac{1}{2}(c_2^2 - c_1^2)] \tag{2.3}$$

While the absolute velocity is of importance for the work done to the fluid, the tangential velocities (c_θ) entering and exiting the compressor show together with the impeller velocity a direct effect on the total work done to the fluid. Usually compressors are run with the flow entering axially, having no swirl component making $c_{\theta 1} = 0$. Pre-swirl, when $c_{\theta 1}$ has a positive value, is when the absolute velocity has a direction not perfectly axial to the impeller but is directed towards the same direction as the impeller rotation, u. Introducing pre-swirl reduces the specific work done to the fluid, but at the same time it reduces the inlet Mach number.

$$\Delta W = u_2 c_{\theta 2} - u_1 c_{\theta 1} = h_{02} - h_{01} \tag{2.4}$$

This energy added to the fluid, $\dot{W}$, is the energy one compares to the energy delivered from a power unit to the compressor to calculate the efficiency of the compressor. In figure 1 the difference in enthalpy between stage 1 and stage 3 equals the energy added to the fluid shown by equation 2.3. Here stage 1 is impeller inlet, and stage 3 is diffuser outlet. It is here some compressor manufacturers make their efficiencies look better by using the different types of enthalpies in figure 1. For example using the static inlet and the total enthalpy at outlet of the diffuser, point 1 to 03, the enthalpy difference results in a better efficiency than if one would use total (stagnation) inlet to total outlet, point 01 to 03.

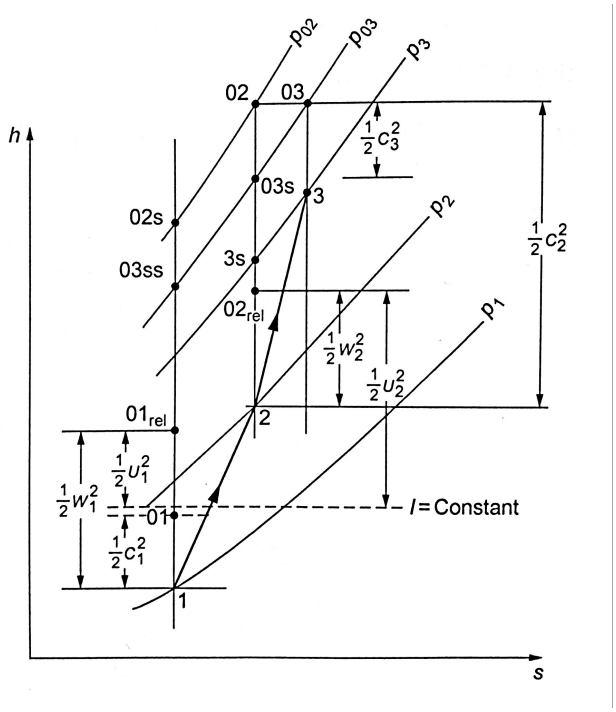

Figure 1: Mollier diagram for a compressor [2].

Figure 2 shows how different geometry of the rotor blades affect the velocity triangle. As shown on the figure, the impeller speed, u_2, is held constant as the relative, w_2, and absolute, c_2, velocities varies. Dixon and Hall [2] discuss the effect on backswept impeller vanes. Effectively concluding in a reduced pressure ratio with an increase in the angle of the vanes relative to radial impeller vanes. At the same time, backswept impeller vanes resulted in a reduced mach number at the impeller inlet. This moves the compressor further away from chocked operation, enabling the possibility of increasing the impeller speed. An impeller with backswept vanes rotating at a high enough speed to match the pressure ratio of a impeller with radial vanes will have a lower Mach number at discharge. This will enable the possibility of higher pressure increase over the compressor, but at the cost of needing a faster spinning impeller. The faster the impeller spins, the more stress is

put on bearings and the blades themselves because of the centrifugal force acting on them as the impeller spins. A common limiter for compressors is the inlet Mach number, as a Mach number of one will result in chocking at inlet. This chocking at inlet dictates the maximum volume flow of the compressor, as it sets a maximum fluid velocity through the inlet which has a fixed cross-section. Splitter blades can be implemented to reduce this limitation at inlet. A splitter blade is usually a blade half the length of a full blade, starting at the midpoint of the impeller and runs down to impeller exit. This in essence results in an increased amount of blades at impeller exit, without limiting the cross section at impeller inlet. When splitter blade are used, usually every other blade is either full length or a splitter. Another advantage with these splitter vanes is better flow guidance, reducing flow separation through the impeller. Figure 2 pictures an impeller solely with full length blades.

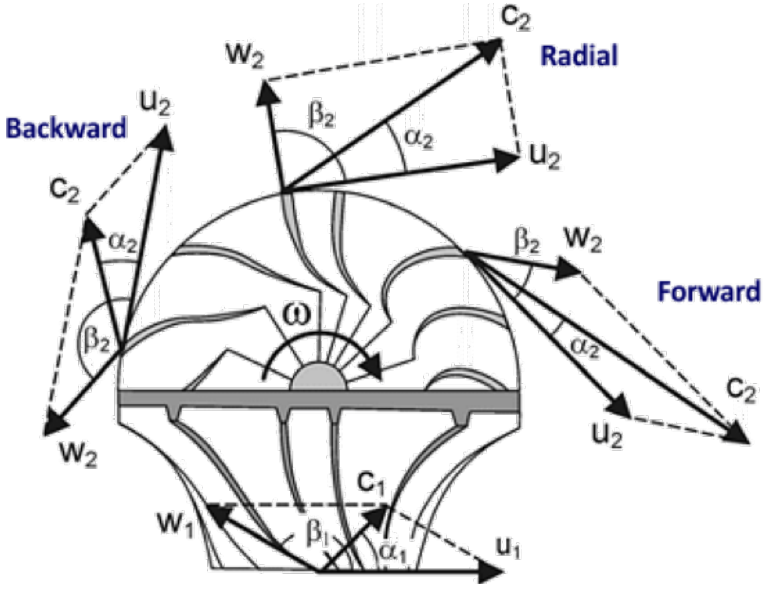

Figure 2: Velocity triangles of a centrifugal compressor with pre-swirl [3].

2.2 Affinity laws

The affinity laws, also known as fan laws, show the relationship between head (H), power (P), volumetric flow rate (Q) and rotational speed (N). These equations show their highest accuracy for low pressure compressors, and are valid under the assumption that the polytropic efficiency is constant.

$$\frac{Q_a}{Q_b} = \frac{N_a}{N_b} \tag{2.5}$$

$$\frac{H_b}{H_a} = (\frac{N_b}{N_a})^2 \tag{2.6}$$

$$\frac{p_b}{p_a} = (\frac{N_b}{N_a})^3 \tag{2.7}$$

These laws can be used to determine compressor behaviour during rundown, by being able to calculate volume flow during rundown based on rotational speed compared to a known operational point [4]. This known point is usually the compressor's normal operating point of which it is being run down from. Combining this with a plot of head versus volume flow enables the possibility to estimate a rundown, or trip, trajectory. These affinity laws will be used to generate compressor curves for 6 000 RPM and 11 000 RPM from the 9000 RPM compressor curves obtained from reference tests. In addition to this, Hysys dynamics utilizes the same laws for it's calculations.

2.3 Trip scenario

A compressor trip is a result of the power unit stopping to deliver power to the compressor. This power unit is usually a gas turbine or an electric motor. A malfunction with the power unit, voltage drops in the power grid (for electric power units) or process related problems upstream or downstream the compressor are examples of events causing trip. When the power unit fails to deliver torque to the shaft connecting it to the compressor the impeller will transfer its energy, as a result of its inertia, to the fluid until it is stopped. This relationship is described by equation 2.8.

$$\frac{dKE}{dt} = \frac{d}{dt}[\frac{1}{2} I_{tot} \omega_c^2] = P_{drive} - P_{fluid} - P_{friction} \tag{2.8}$$

This is often referred to as the fluid's breaking effect on the impeller. The breaking effect is dependent on the size, weight and rotational speed of the impeller, gas density, gas pressure and volume flow. Under these transient conditions pressure ratio and volume flow will decrease, and for larger systems in a manner which could result in the compressor going into surge. The behaviour of a compressor during trip is often illustrated by plotting its operational point in a pressure ratio vs volume flow graph over time. This line is referred to as the trip trajectory or trip route.

2.4 Compressor surge

The main objective behind investigating how a compressor behaves during a trip is to understand how to avoid surge. Figure 3 shows a typical compressor operating diagram with polytropic head over volume flow. Each of the downward turning lines represents a constant rotational speed for the compressor. The line marked "SL" refers to the surge line. In essence surge can be described as a situation where the compressor is not able to deliver sufficiently high pressure ratio at a given flow rate to push the fluid through the compressor in the normal operational direction. This in turn leads to back-flow in the compressor, which in turn results in a higher pressure at inlet. This reduces the pressure ratio and enables the flow to move in the correct direction again[5]. This results in an oscillating flow and is what makes surge potentially damaging for the equipment.

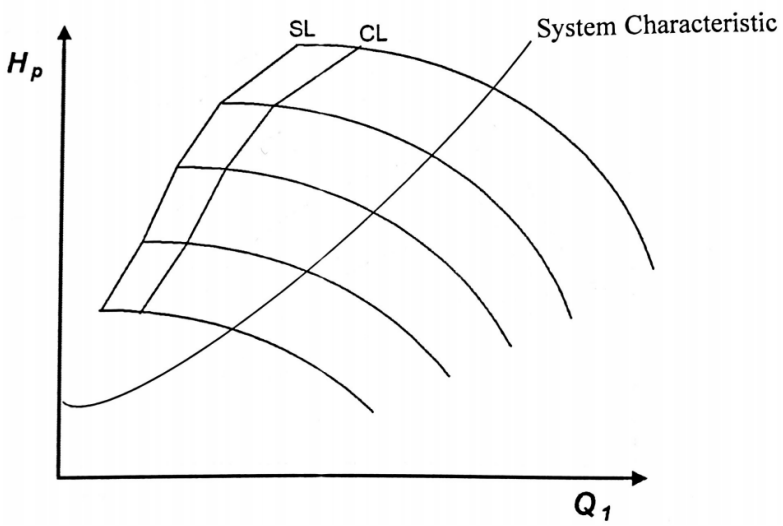

Figure 3: Compressor operating diagram [2].

When a compressor goes into surge, the oscillating flow can generate violent vibrations in the compressor unit, thus damaging it. Because of the potential costly consequences of letting a compressor go into surge, most industrial compressors feature an anti-surge system. The simplest version of such a system is a hot gas bypass, which enables the possibility to recirculate fluid from compressor exit to compressor inlet. This recirculation increases the volume flow through the compressor and shifts the operational point to the right in figure 3, thus avoiding surge. A hot gas bypass is more of a last resort, for example during trip, as recirculating hot fluid multiple times can quickly increase fluid temperature well outside safe operational conditions. The solution to this is to use a anti surge valve which in essence is a hot gas bypass with after-cooling. As a result of the longer loop with

after-cooling, the anti surge valve has a longer response time. Both of these systems waste a considerable amount of energy when active, and should not be used under normal operation. When the gas feed is limited, for example during start up, the anti surge valve is used to supply the compressor with sufficient gas flow over a sustained period to keep it operational. Figure 4 shows how these systems are implemented for the Troll Kollsnes pipeline compressor.

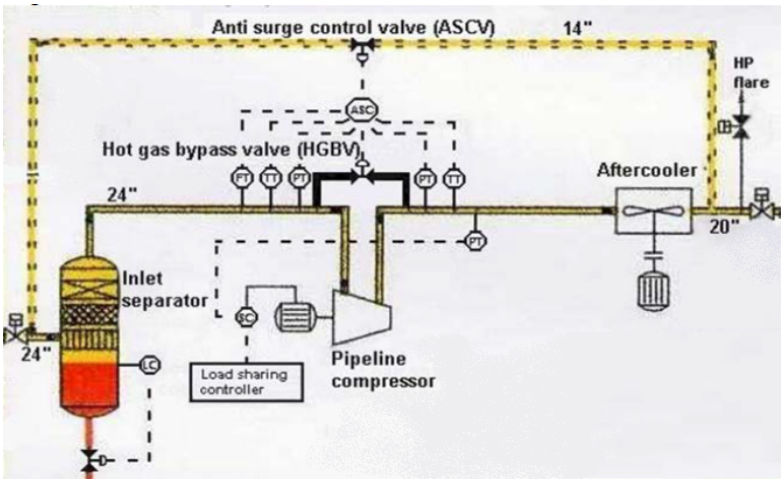

Figure 4: Overview of Troll Kollsnes pipeline compressor process[6].

The response time is, as mentioned, of great importance for a surge preventing system. L.E Bakken et al.[6] studied how the Troll Kollsnes natural gas pipeline compressors behaved during trip and how various conditions and systems affected run-down of the compressors. For the Troll Kollsnes plant a dip in power lasting 150 milliseconds could be sufficient to force the compressors to trip. From that it takes under half a second for the compressors to go into surge as shown in figure 5.

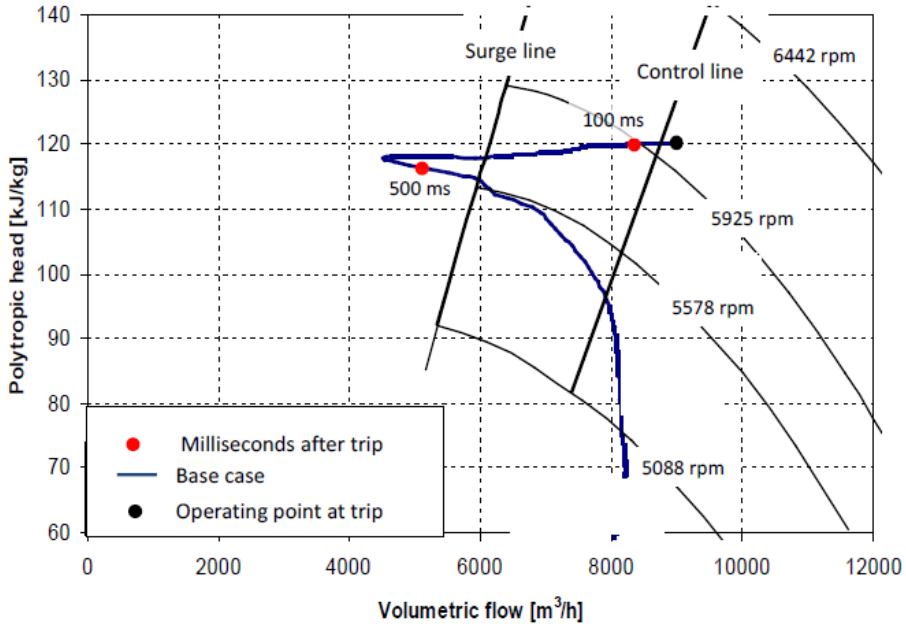

Figure 5: Troll Kollsnes base trip test [6].

As a trip could send the compressor into surge so quickly, the safety systems must be able to act in a similarly rapid manner. Figure 6 shows how different hot gas bypass valves affect the rundown-path of the compressor, and that all three of the hot gas bypass systems manages to keep the compressor away from surge.

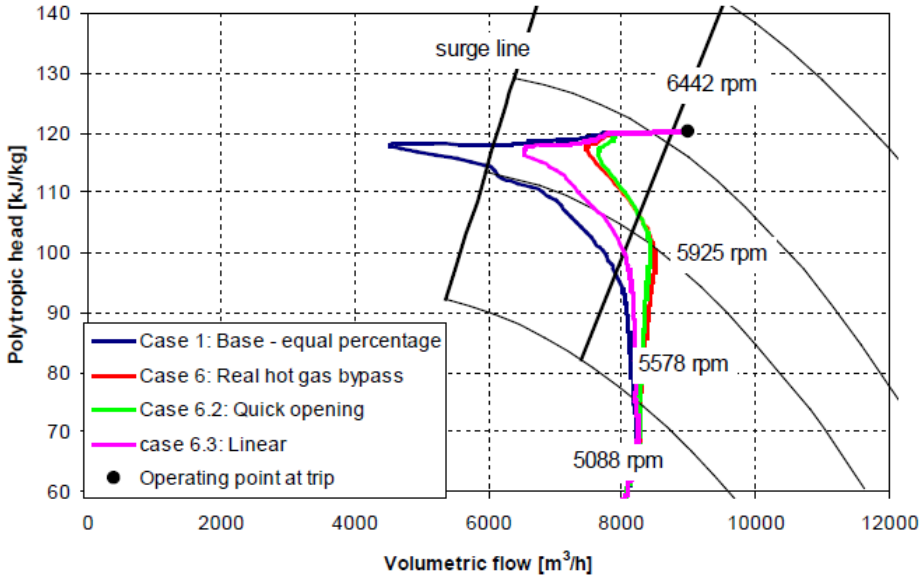

Figure 6: Troll Kollsnes different hot gas bypass valves trip test [6]

2.5 NTNU compressor test facility

The compressor test facility located at The Department of Energy and Process Engineering at NTNU Trondheim has been used in this project. This rig consists of a shrouded impeller with a vaneless diffuser that work an open loop with the possibility for water injection. Driving the compressor is a 450 kW electric motor, enabling the compressor to operate at a maximum rotational speed of 11 000 RPM. This motor is controlled by a variable speed drive, and is connected to the compressor shaft with a torque meter in between.

All instrumentation has been installed in accordance with ASME PTC 10. Hydraulic valves at inlet and outlet can be used to regulate the gas flow rate, which in turn is measured by an orifice plate mounted in the inlet pipe well upstream of the compressor to provide uniform flow over it.

Variable	Instrument accuracy	Unit
Ambient temperature	± 0,2	°C
Ambient pressure	± 0,15	hPa
Relative humidity	± 1	%
Temperature flow element	± 0,15	°C
Pressure diff. flow element	± 0,04	%
Inlet pressure, compressor	± 0,3	%
Inlet temperature, compressor	± 0,005	°C
Outlet pressure, compressor	± 0,3	%
Outlet temperature, compressor	± 0,006	°C
Shaft speed	± 5	%
Shaft torque	± 0,05	%

Table 1: Instrument accuracy of the NTNU compressor rig

The compressor rig uses a data acquisition system based on a National Instrument PXI, capable of stable measurements with a sampling frequency of up to 20 kHz. The inlet piping just upstream of the compressor is made of plexiglas as well as the diffuser and volute section, enabling the possibility to observe the flow characteristics for multiphase flow. For a more detailed rig description, see Hundseid et al [7].

2.6 Aspen Hysys

The Aspen Hysys Dynamics process simulator is a full scale plant simulation program using first principle thermodynamic, mechanical and chemical relationships. Ordinary differential equations representing conservation relationships for mass, components and energy are solved continuously using the Implicit Euler Method. In turn this results in the possibility of accumulation within the process equipment, a crucial part of the dynamic analysis. The program is widely used in the petroleum industry and can utilize a vast variety of equations of state in order to cope with various fluids and conditions. Hysys dynamic will be used in all compressor simulations in this thesis.

3 Air to hydrogen gas conversion procedure

Hydrogen gas is highly flammable, resulting in safety concerns for testing and developing centrifugal compressors for the fluid. There is therefore an incentive to develop a procedure for relating a compressor's performance on compressing air to it's performance when compressing hydrogen gas. The properties of the two different gases vary in areas which are difficult to account for, somewhat limiting the achievable accuracy of this method. The compressor might for example be able to run at higher RPM with hydrogen gas than with air as a consequence of hydrogen's high sonic velocity.

3.1 Compressor performance characteristics for air

The Department of Energy and Process Engineering's own wet gas compressor rig was used to establish compressor curves for dry air. All measurements were done according to ASME PTC-10 and ISO 5167. These reference test were conducted in collaboration with fellow NTNU student Knut Erik Ellingsgård Johansen. After consultation with supervisor, risk analysis and description of the test procedure can be found in Knut's Master's thesis: Subsea Compressor Transients. The results from the two reference tests can be found in the appendix.

The compressor was set to run at 9000 RPM, and the volume flow was regulated by a valve placed far away from the inlet of the compressor itself. As the environment in which the compressor is placed is not particularly easy to regulate, the compressor had to run for a extended period to achieve a satisfying degree of thermal stability. After testing, the results were compared to Aspen Hysys and were reasonably coinciding.

The test was started to the far left in figure 7 with the compressor close to surge before increasing the volume flow all the way to chocked operation. This was done to help with the thermodynamic stability of the compressor, as moving from low to high volume flow helped reduce the temperature difference over the different readings. Thermodynamic stability for this open loop compressor rig was defined as a lower than 0,2 °C temperature increase at inlet over 15 minutes of compressor operation.

The ASME PTC10 standard gives the requirements for performance testing of different fluids and

test conditions. A detailed evaluation of given requirements between air and hydrogen gas is outside this thesis scope of work and is therefore not included.

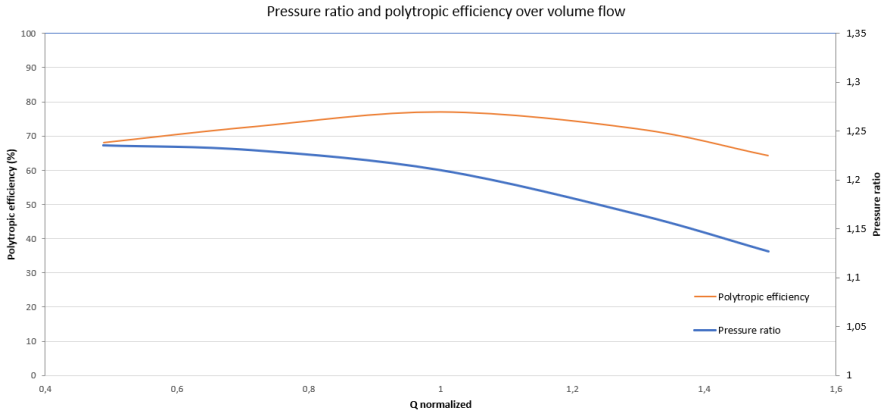

Figure 7: Pressure ratio and polytropic efficiency over volume flow for air

3.2 Assuming constant polytropic head

The simplest way of relating the compressor's performance on the two fluids is to assume that the compressor manages to deliver the same amount of energy to the two fluids, i.e polytropic head, and relate that to the pressure ratio. This method also assumes equal polytropic efficiency for both fluids, and that the polytropic exponent stays constant.

To do this calculation, the polytropic head has to be calculated for the compressor while working on air.

$$H_p = \frac{n_v}{n_v - 1} \frac{Z_1 R_0 T_1}{M} [(\frac{p_2}{p_1})^{\frac{n_v - 1}{n_v}} - 1] \tag{3.1}$$

Using values from the compressor reference test number 1, with the compressor running at 9000 RPM and varying the inlet valve from 30 % to 100 % the polytropic head for air is calculated with equation 3.1. This polytropic head is then used to calculate the pressure ratio for hydrogen by reorganizing the equation to 3.2.

$$(\frac{p_2}{p_1}) = [\frac{H_p(n_v - 1)M}{n_v Z_1 R_0 T_1} + 1]^{\frac{n_v}{n_v - 1}} \tag{3.2}$$

Thermodynamic values for the calculations were found using Hysys for air and mini-REFPROP version 10.0 [8] for hydrogen. The full spreadsheet of the values used can be found in the appendix.

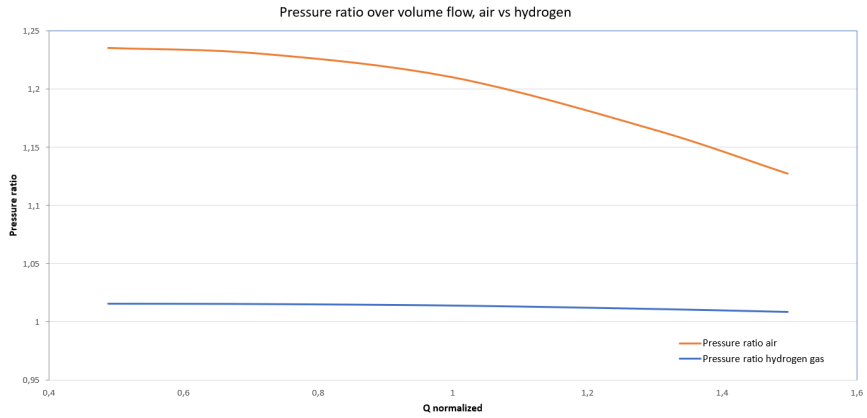

Figure 8: Pressure ratio for air and hydrogen gas

The graph shows that even though the pressure ratio for air is relatively low, the ratio for hydrogen is so small that the variations over volume flow almost vanishes.

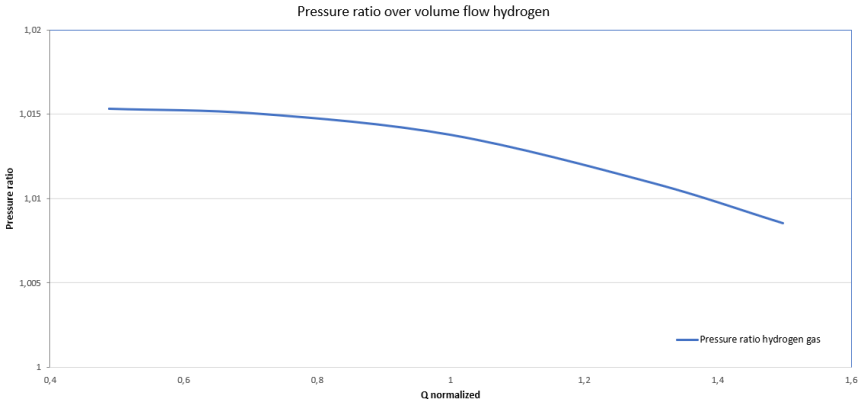

Figure 9: Compressor curves showing pressure ratio for hydrogen gas

As a result of hydrogen gas' low molecular weight the pressure increase is drastically lower than for air, so low that the compressor is well under the pressure ratio defined for a fan. This basically results in the need for a higher energy input to reach a given pressure, increasing the operational cost of a hydrogen compressor. Additionally it results in a even bigger than normal incentive to

have high efficiency compressors for hydrogen gas, as each percent point of increased efficiency will result in larger absolute energy savings. This high need for energy to increase pressure is fluid dependant, thus inevitable.

At best efficiency point (Q normalized equal to 1) one would need at least 13 of the same compressor in series to manage the same pressure increase for hydrogen gas as one compressor achieves with air. This small pressure ratio for hydrogen also imposes another challenge as a small change in pressure ratio results in a huge change in volume flow, as shown in figure 9. In turn this would, if the pressure ratio over the compressor is sufficient, make the compressor highly vulnerable to surge.

3.3 Reynolds correction

In chapter 3.2, the polytropic efficiency of the compressor was assumed equal for hydrogen as it was for air. The reasoning behind this was the low impact it had on the calculations of pressure ratio. For instance, setting the efficiency to 0,3 for the lowest flow point from the reference test (30 % valve opening) resulted in a reduction in discharge pressure in roughly a tenth of a millibar (without accounting for an increase in hydrogen discharge temperature which would affect the polytropic exponent somewhat).

The International Compressed Air and Allied Machinery Committee (ICAAMC) published in 1987 a paper on Reynolds correction; "Influence of the Reynolds Number on the Performance of Centrifugal Compressors" [9]. This paper highlighted the variation of the Reynolds number between workshop tests and specified conditions and how this affected performance for compressors, especially centrifugal compressors.

Firstly, some assumptions had to be made. Mean flow velocity in the flow channels of a compressor stage is approximated to half the tip speed of the impeller and the mean hydraulic diameter is to twice the outlet tip width resulting in:

$$Re = \frac{\frac{u_2}{2} 2b_2}{\nu} = \frac{u_2 b_2}{\nu} \tag{3.3}$$

A Moody diagram can be used to find friction factors, but the von Karman equation for friction factor at Reynolds number (3.4) and the Colebrook equation for friction factor at specified (3.5) and test operating (3.6) conditions are generally accepted. The Moody diagram [10] can be found in the appendix.

$$\frac{1}{\sqrt{\lambda_{cr}}} = 1,74 - 2log_{10}[2\frac{R_a}{b_2}] \tag{3.4}$$

$$\frac{1}{\lambda_{sp}} = 1,74 - 2log_{10}[2\frac{R_a}{b_2} + \frac{18,7}{Re_t\sqrt{\lambda_{sp}}}] \tag{3.5}$$

$$\frac{1}{\lambda_t} = 1,74 - 2log_{10}[2\frac{R_a}{b_2} + \frac{18,7}{Re_t\sqrt{\lambda_t}}] \tag{3.6}$$

Solving for the three friction coefficients in the equations or reading the values off a Moody diagram enables the use of the formula proposed in the paper by ICAAMC. Note that the efficiencies η_{sp} and η_t are polytropic efficiencies at specified and test operating conditions.

$$\frac{1-\eta_{sp}}{1-\eta_t} = \frac{0,3+0,7\frac{\lambda_{sp}}{\lambda_{cr}}}{0,3+0,7\frac{\lambda_t}{\lambda_{cr}}} \tag{3.7}$$

The only fluid dependent variable used here, kinematic viscosity, alters the Reynolds Number for both of the Colebrook equations. Using hydrogen's kinematic viscosity for calculating values for the specified operating condition and air's kinematic viscosity for the test operating condition the Reynolds corrected efficiency can be found. The correction is valid as long as the remaining ASME PTC10 requrements are fulfilled.

3.4 Increasing pressure ratio for hydrogen compressors

As hydrogen gas is dependent on being highly compressed to be able to compete with petroleum products as an energy carrier, centrifugal compressors have to be able to reach a high pressure ratio. As the compressor test on air, with the following conversion to hydrogen gas, highlighted that this could be a major challenge. Following are some methods of increasing the pressure ratio of centrifugal compressors.

For an existing compressor rig there are not many options to do so. The first will be to limit the flow to the compressor, moving the operational point higher up on the compressor curve. A major downside to this is that the safety margin to surge which the compressor is designed to operate with is decreased. Additionally, this reduces the amount of gas processed per time by the compressor. The gain in pressure ratio by using this method also has a somewhat limited potential and will move

the operational point away from the best efficiency point. Increasing the rotational speed will also increase the pressure ratio, along with decreasing the efficiency and durability of the compressor. This is illustrated in figure 10, where the further the operational point is away from the centre of the dotted circles the lower the efficiency.

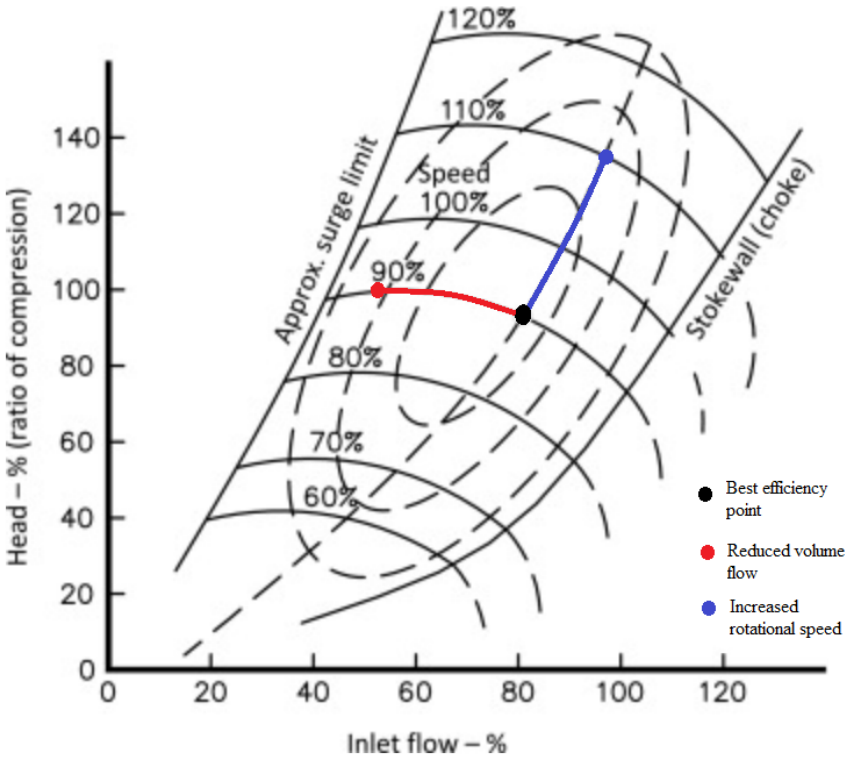

Figure 10: Centrifugal compressor performance map [11].

When a compressor is designed, blade angles and rotational speed are matched up with each other do reach the desired pressure ratio. For high pressure ratios multiple stages with inter-cooling is used to counter the increase in temperature a gas experiences during compression. Increasing the rotational speed of a compressor stage will result in a higher pressure increase over it, to a degree, until chocked operation is achieved. As a result of the gas having the lowest temperature at inlet, this often is where chocking occurs. The reason behind this is the role of which temperature plays for a gas' sonic velocity. In essence sonic velocity is how fast sound waves are able to travel through the fluid. This velocity is then the same as the velocity at which the fluid can travel without the risk of sonic shocks, or in compressor terms; choking. For hydrogen gas this sonic velocity is rather high,

1270 m/s at 20 °C. Most common gases used in petroleum industry like methane, propane and carbon dioxide lie in the 250 to 450 m/s range at the same conditions. This trait of hydrogen could be exploited to manage higher pressure ratios for centrifugal compressors working on hydrogen gas.

The American-based company Mohawk Industries have done research on such a high RPM compressor for hydrogen gas, shown in figure 11. Helium was used as a substitute gas for the experiments.

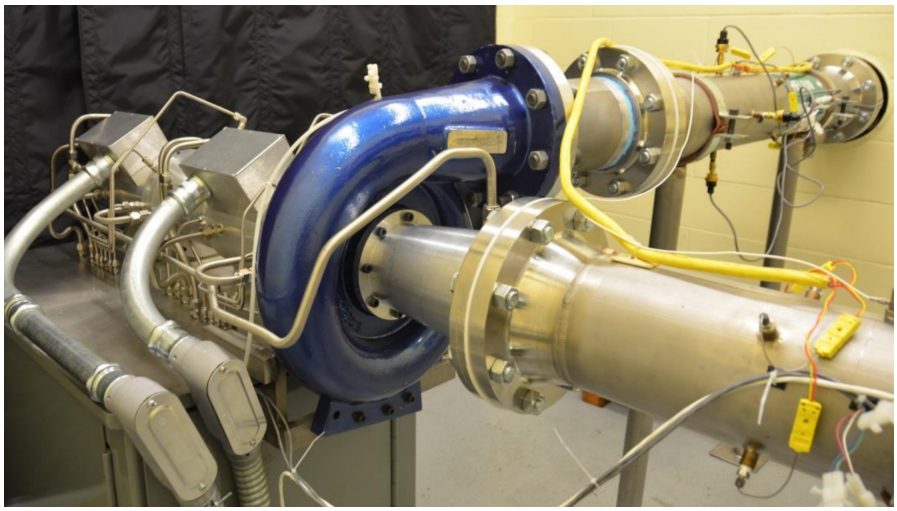

Figure 11: Mohawk Industries modular single stage test rig [12] .

The Mohawk Industries' impeller, shown in figure 12, has some interesting features. The first thing to notice is the amount of blades and how closely spaced they are. Considering that this impeller rotates at 40 000 RPM, this design would risk being limited by chocking at impeller inlet if not hydrogen/helium had such a high sonic velocity. Especially since all blades on the impeller are full length, and there are no splitter-blades. In addition to this, the blade angle at impeller exit is fully radial, indicating that the sonic velocity neither is an issue at impeller exit. An interesting possibility here is that there might be enough headroom regarding the sonic velocity at impeller exit to use forward facing blades, as this would result in a higher pressure increase over the compressor stage at a given impeller speed.

Figure 12: Mohawk Industries impeller[12].

4 Compressor trip

The electrification of the Norwegian oil and gas production is a step in the right direction regarding de-carbonisation of the energy producing industry. Compressors and pumps can, and are for new installations legislated to, be driven by electric power units instead gas turbines. With this comes the possibility to more easily regulate compressor speed, less power usage and of course lower emissions. However, with an electric power unit follows some challenges. Most of these challenges originate from the dependency on the electrical grid. Small and momentary drops in voltage can for a electric power unit in the two digit megawatt range result in tripping of the whole compressor system [6]. This trip can in some instances result in the compressor going into surge, possibly damaging the unit. Hydrogen gas, for example from electrolysis of water, is one of the main contenders to substitute natural gas. There is therefore an incentive to investigate how a compressor behaves during trip (referred to as trip trajectory or trip route) while compressing hydrogen gas. A dynamic model in Hysys Dynamics was provided by M.Bakken [13], slightly modified and verified for the NTNU wet gas compressor rig running on air before simulating the different situations for hydrogen gas.

4.1 Reference trip tests

The reference trip tests were done in two different ways; with a standard trip, and with regulation of the compressor's outlet valve during trip. The latter of the two was to simulate the trip-behaviour of a larger, higher pressure ratio, compressor as it prolongs the pressure drop during trip at discharge. These tests are the baseline to which the Hysys model will be compared to.

A surge line was made based on the results from the non-trip reference tests used earlier. As the surge line is based on only one compressor curve, therefore it is only viable for operation at 9000 RPM. In addition to this, the non-trip reference tests were done at conditions close to thermal equilibrium for the environment of the compressor, resulting in the starting point of the trip test not to lie at Q and dP normalized equal to one.

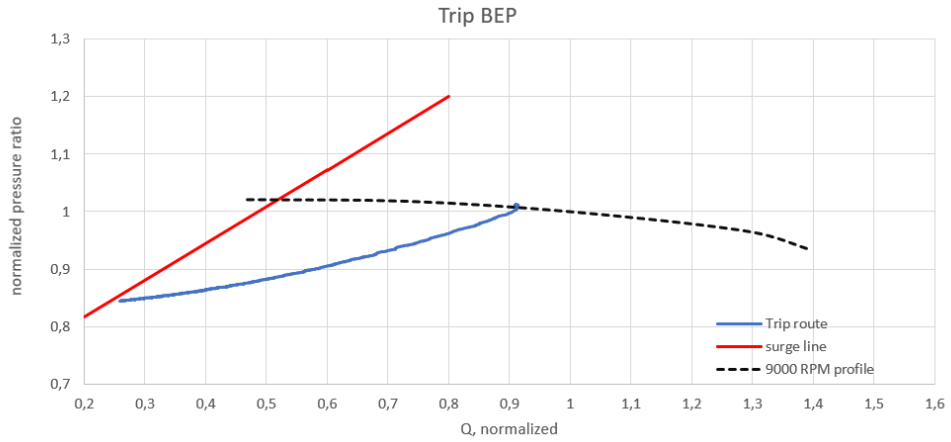

Figure 13: Compressor trip from BEP

Figure 13 shows a plot of the trip trajectory together with the compressor's 9000 RPM profile and a surge line (surge line from the Doctoral thesis of M.Bakken [13]). The trip trajectory starts at the 9000 RPM profile, is logged at 20 hertz and for roughly 60 seconds. One interesting behaviour of the compressor is that for the first half second of the trip the trip trajectory is straight downwards, indicating constant volume flow rate while pressure decreases. This was initially thought to be a result of the pressure sensors' short response time and the fact that the flow measurement is done some distance from the compressor. At such low pressure as in this experiment air can be considered to be close as incompressible. Additionally, the pipe between the point of flow measurement and pressure measurement is not sufficiently long to result in this delay. The delay was found to be of such a consistent manner that it was concluded with being a signal delay originating from the

sensors and/or the processing unit.

For the whole duration of the trip the compressor stays well outside of surge. This compressor does simply not have the pressure ratio needed to make it able to surge. To be able to simulate the trip of a larger compressor the exit valve was regulated in such a way that the discharge pressure was kept higher for a longer period after trip. How this was implemented is described later in the thesis.

The closing of the discharge valve (ramping) at trip showed that the compressor did in fact behave more in line with one of a larger system. The valve was programmed to close from 54% to 30% over a three second period, hold at 30% for one second before reopening to 54% in the same manner as it closed.

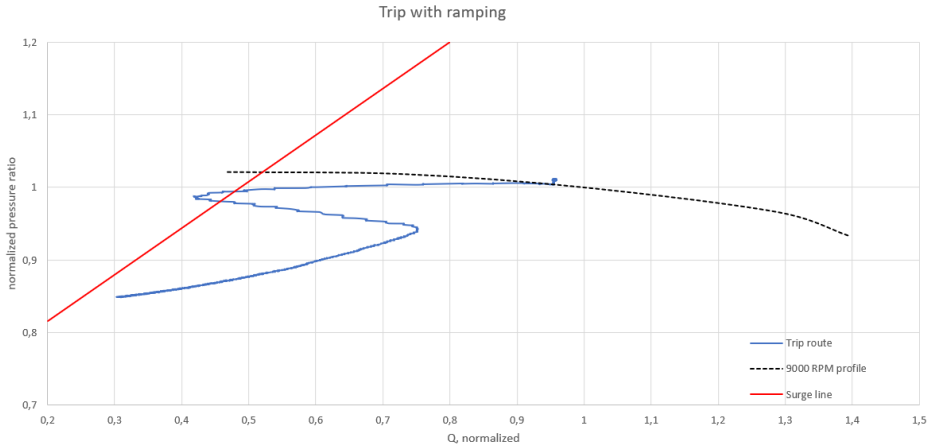

Figure 14: Trip with discharge valve ramping

Figure 14 shows that the ramping had sufficient effect on the compressor to force it into surge, at least for a short period. This is evident by the trip route crossing the surge line. Additionally, the trip route is not particularly smooth, something that might be a consequence of the manner of which the discharge valve closes. Figure 15 shows a similarly uneven closing/opening of the valve as the route of the trip during valve ramping. This might indicate that the uneven valve movement generates small oscillations in pressure and volume flow which propagate through the system.

4.2 Tuning of the Hysys-model

The accuracy of the Hysys-model is of great importance. The discharge valve, used to force the compressor into surge at trip, initially caused some problems for the simulation. In the experiments the valve was set to 54% opening before trip, which was determined by the reference tests to be the best efficiency point. When trip was initiated the valve was supposed to use three seconds down to 30% opening and stay there fore one second before returning to 54% over the same three second period. When working with the simulation, the valve was regulated in the same manner. When plotting the behaviour of the valve in the experiment versus the simulations there are some considerable deviations when the valve was simulated as specified by valve's data-sheet (1,5 seconds actuator time constant and 0,7 seconds valve stickiness time constant). This was a result of the ramping which the valve was programmed to, which made it deviate from it's data-sheet.

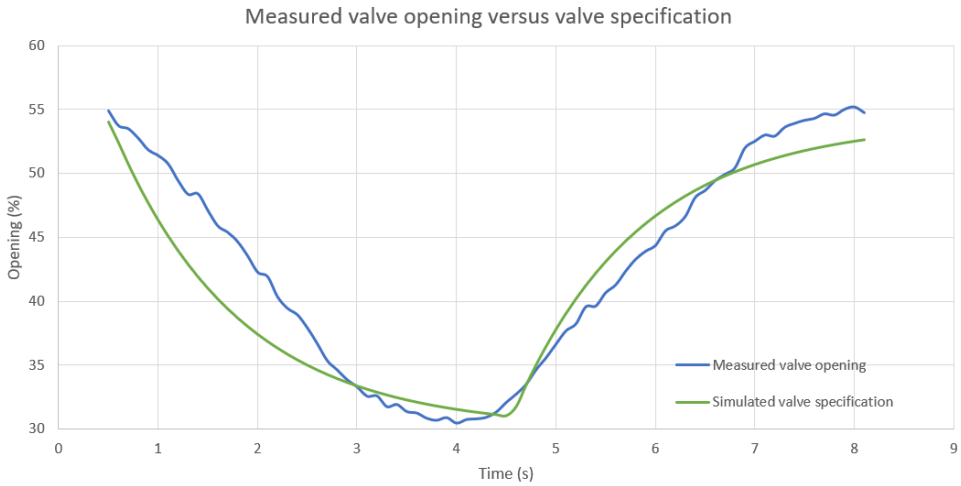

Figure 15: Comparison of simulated and measured valve opening

In figure 15, the blue line shows how the actual valve behaved during tests, and that it behaved in a non-ideal manner. For example the starting point was 0,9 percentage point above the set-point. Additionally, it did not manage to transition from 54% to 30% opening in the required 3 second period. Instead the valve reached around 31% opening for roughly 0,75 seconds before starting to open again. The simulated version of the valve, with the specifications from the data-sheet, did not replicate this behavior in a satisfactory manner. This can be seen in figure 15 where the green line represents the simulated valve, and how it in some periods deviates with up to five percentage points from the actual valve. Rather than using the valve specifications from the valve's data-sheet in the simulation, the decision was made to regulate the simulated valve to approximately behave

as its real-life counterpart.

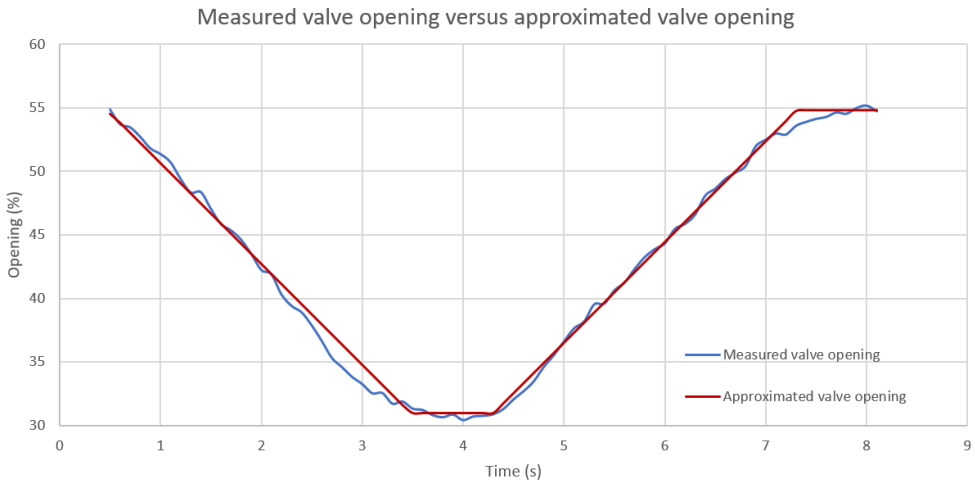

Figure 16: Comparison of approximated and measured valve opening

Figure 16 shows the behaviour of a simulated valve with a linear actuator rate of 8% per second, a holding time of 0,75 seconds and a lower set-point of 31%. Additionally, the valve has a starting and ending set-point of 54,5%. This resulted in the simulation behaving much more similar to the real-life test. This setup for the discharge valve was used in all simulations.

The method for determining the accuracy of the simulation was to input the atmospheric conditions for the reference test and compare the simulation's output to the reference test at a given compressor speed. Table 2 shows how the simulation deviates from the reference test, and that for the most part the simulation has a high accuracy. All values in the figure are for the compressor running at 9000 RPM and with a discharge valve opening of 54,5 %.

The Hysys model was originally tuned to the NTNU wet gas compressor by M.Bakken, but the rig had underwent some changes regarding the inlet pipes and a water injection manifold had been removed. This lead to inaccuracies in the temperature and pressure at compressor inlet at a given set of ambient conditions. The compressor rig inlet pipe length was measured, and some minor adjustments to the length and material of the inlet pipe of the model were done. This affected the pressure loss and friction generated heat of the inlet pipe so that the model's accuracy reached an acceptable level.

Variable	Ref.test	Simulation	Deviation (%)
Rel.humid (%)	**36,3**	**36,3**	**0**
P_atm (mbar)	**974**	**974**	**0**
T_atm (C)	**26,45**	**26,45**	**0**
P_inlet (mbar)	932,25	928,5	-0,404
T_inlet (C)	27,58	27,62	0,145
P_outlet (mbar)	1126	1112	-1,259
T_outlet (C)	48,1	49,82	3,452
Dp_orifice (mbar)	41,9	37,2	-12,634
Comp Torque (Nm)	30,5	30,6	0,327
Mass flow (kg/s)	1,2845	1,2833	-0,094
Volume flow (m^3/s)	1,1892	1,1989	0,804
Pressure ratio (-)	1,2078	1,1976	-0,852

Table 2: Comparison of data of reference test and simulation

The largest difference between the real and simulated values is for the pressure drop over the orifice ("Dp_orifice"). There are two reasons to this; the small pressure drop over the orifice results in a large difference in percentage at a small real difference, and the orifice is modelled as a regular valve with similar specifications as the real orifice. For the compressor rig the orifice is used to measure volume flow via the pressure drop over it, but for the simulation its main purpose is to act as a restriction in the inlet pipe as Hysys does not use the orifice to measure the volume flow. As the deviance in volume flow for the reference test and the simulation is considerably smaller, the inaccuracy of the pressure drop over the orifice is found to have a low impact on the total accuracy of the model and is therefore acceptable.

The temperature at outlet is noticeably higher for the simulation than the reference test. In reference test number 1 prior, the outlet temperature was under 46 °C. This was before the position and mounting of the temperature sensors were changed, and reference test 2 was conducted. The sensor was believed to not reach far enough into the pipe, and the metal mounting to conduct heat away from the sensors and out to the ambient air outside of the pipe. It is a possibility that the sensors still underreport the temperature at outlet.

4.3 Dynamic model trip comparison

In this chapter the accuracy of the Hysys model during trip will be investigated by comparing the trip trajectory/route of the simulations to the trip reference tests.

Comparing the compressor to the model at stable conditions is relatively straight forward, but a trip is not an event where the compressor operation is everything but stable. The Hysys-model was set to mimic the reference trip tests as closely as possible in terms of conditions before trip and operation of the discharge valve, when relevant. This would in an ideal world result in the trip route of the simulation to be identical to that of the reference trip test. Figure 17 shows the simulated trip route. At first glance it seems to follow the same trend as the actual trip route.

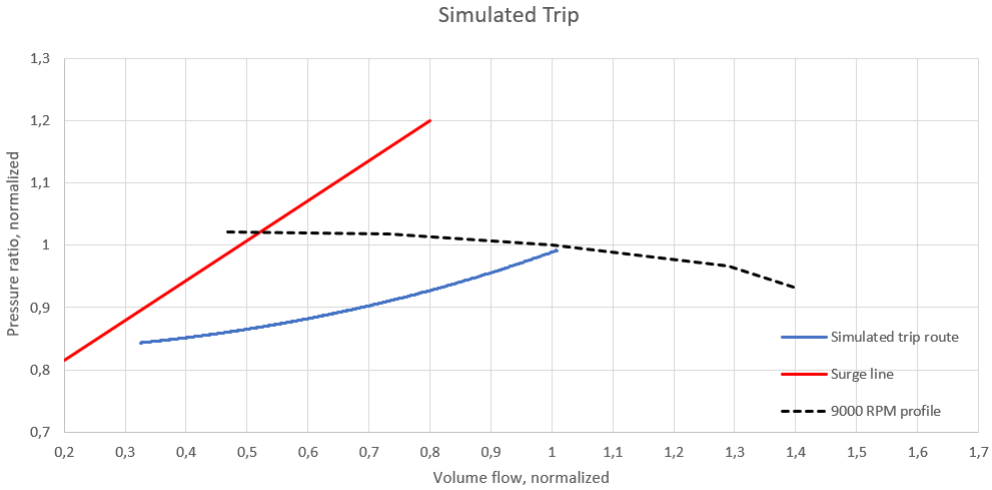

Figure 17: Simulated trip

One thing to notice is that the starting point of the trip is closer to point (1,1), BEP, than the actual trip tests were. This is a consequence of the Hysys-model being optimized at stable BEP conditions. This was made clear by plotting both the simulated and the actual trip in the same graph.

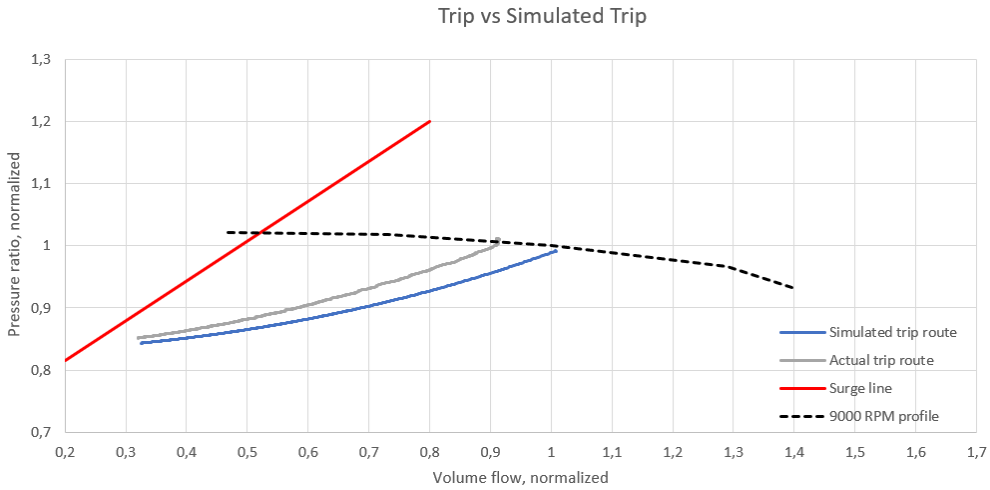

Figure 18: Simulated trip vs actual trip

The stable operational point just before trip is initiated is dependent on various parameters like the humidity, temperature and pressure of the ambient surroundings. Variation in these parameters between the reference tests and the trip tests can explain much of the differences between the starting point of the simulated trip and the real life one. To give a better visualization of how the model behaves compared to the real compressor, the simulated trip route was adjusted in such a way that the simulated trip and the actual trip had the same starting point. The adjustment made to the starting data point of the simulation was also made, in an absolute manner, to all other data points. In other words; every data point of the "simulated trip route"-line was moved upwards and to the left in the diagram so that the starting points of the simulated trip and the actual trip would coincide. The actual trip shows some unexpected behaviour with constant volume flow with decreasing pressure ratio, which will be discussed later on. To avoid this unexpected behaviour affecting the comparison of the two trip routes, the starting point of the actual trip has been set to the point where both pressure ratio and volume flow starts to decrease. This illustrated better how the simulated trip compared to the actual trip's behaviour.

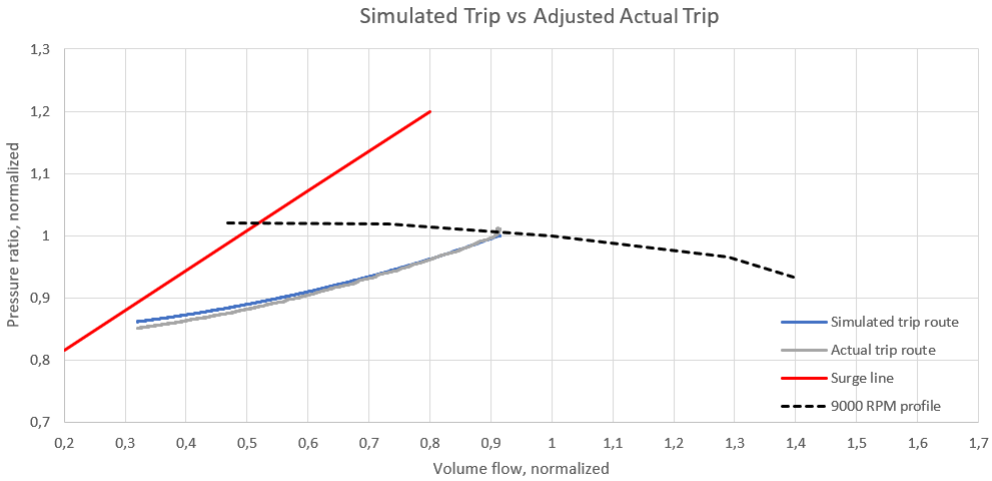

Figure 19: Simulated trip vs adjusted actual trip

As mentioned before this compressor system is not of sufficient scale to naturally risk going into surge during a trip and ramping of the discharge valve is used to force the compressor into surge. This type of operation is of a more complex manner, making it less likely for a model to simulate accurately. The simulated operation of the discharge valve was implemented as described by the "approximated valve opening" in figure 16. The real life trip route is adjusted in the same manner as before, to eliminate the variances in steady operation as a consequence of changing atmospheric conditions.

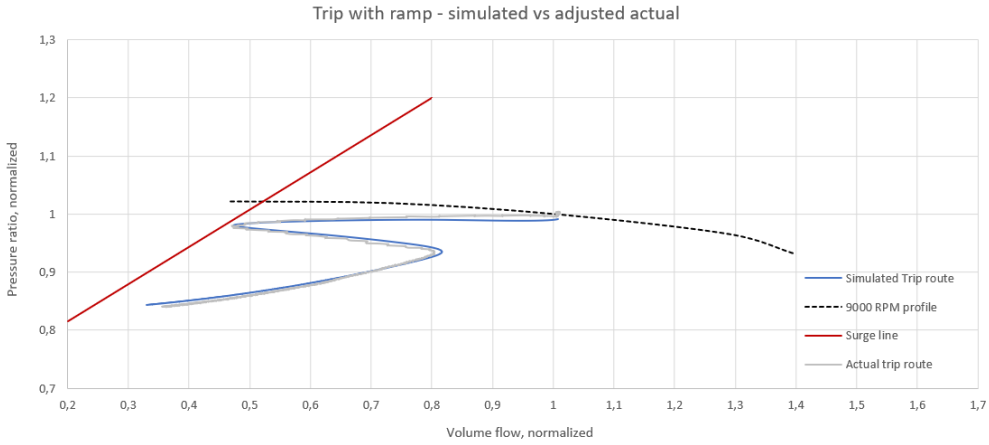

Figure 20: Simulated vs adjusted actual trip route with ramping

Once again the model simulates the behaviour of the compressor quite accurately when adjusted. One thing to notice is that the uneven curve of the actual trip route is not reproduced in the simulation, somewhat strengthening the theory that the discharge valve itself is producing these oscillations. The initial behaviour of the actual trip where the pressure ratio drops, without reduction in volume flow is not replicated by the model. This pressure drop at constant volume flow is also present at the simple trip without ramping, excluding the closing of the discharge valve as the reason to this initial behaviour. Volume flow is measured by an orifice which is placed almost at the very start of the roughly 35 meter long pipe leading up to the compressor, while the pressure sensors are placed within a meter of the impeller. This will result in a higher responsiveness of the pressure sensors than of the orifice. This delay is dependent on the how the change in energy propagates through the gas, which will equal the speed of sound of the gas. As the speed of sound in air at 25 °C is over 345 m/s this will result in a delay of about a tenth of a second, not in the 1 to 2 second which is the case here. It is also worth noting that the actual trip route did cross the surge line before adjustment, as shown in figure 14. Upon further investigation a signal delay for the orifice became evident as it was relatively consistent in all tests. The simulations for both the simple trip and the trip with ramping had satisfying levels of accuracy when accounting for changes in ambient conditions.

4.4 Trip and blockage at 9000 RPM

Another interesting situation to simulate would be a trip with a close to total blockage of the discharge pipe. A malfunctioning valve or the need to instantly shut down the compressor to prevent damage to equipment downstream in the facility can be situations where the compressor will have to trip while the discharge pipe is more or less blocked. Pressure will build up at compressor exit and, if not vented, will start to back-flow. As this can be quite damaging to the compressor it is worth taking a look at. Additionally, it is interesting to find out how the accuracy of the Hysys model is in this situation. The simulation was initially done with total blockage, 1 % , 2,5 % and 5 % valve opening where all situations resulted in the compressor going into surge. Back-flow was present at all simulations except the simulation with 5 % opening. It was decided to focus on simulating compressor trip with full blockage. The discharge valve of the NTNU compressor rig does not have the ability to close fully shut, but it is still an interesting situation. At trip the discharge valve was set to close with the parameters from its data sheet, not the 8 % per second rate from figure 16, since it now was simulating the valve closing at it's maximum rate.

The first simulation, with the discharge valve closing all the way, yielded some promising results as it showed an oscillation between positive and negative flow, typical for a compressor in surge. A compressor would highly likely run into surge if put in this situation, initially indicating believable behaviour. Figure 21 shows how the flow varies between positive and negative flow as pressure slowly decreases, in such a manner that the blue line in the graph almost covers the white background. This behaviour will be referred to as "full surge". The graph as a whole is rather messy with the full surge section close to covering the rest of the graph and thus does show much more than this typical surge pattern.

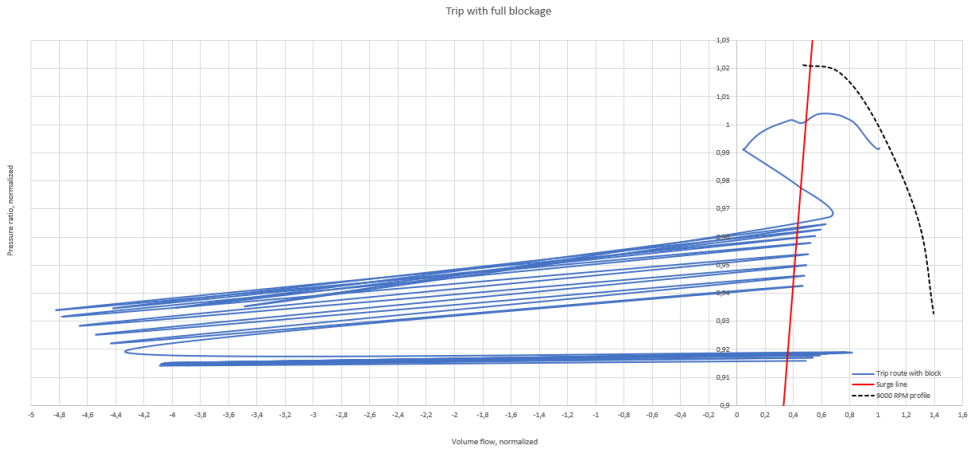

Figure 21: Full trip with blockage, 9000RPM, 10hz

A quite interesting observation is that the first 4,5 seconds represented in the graph is from the starting point just beneath the 9000 RPM profile and to the point where the graph turns sharply down and to the right before crossing the y-axis. In the following 0,5 seconds the compressor moves into full surge. To look closer at the moments between trip and full surge sampling frequency was increased to 100 hz, and just the first 5 seconds were plotted.

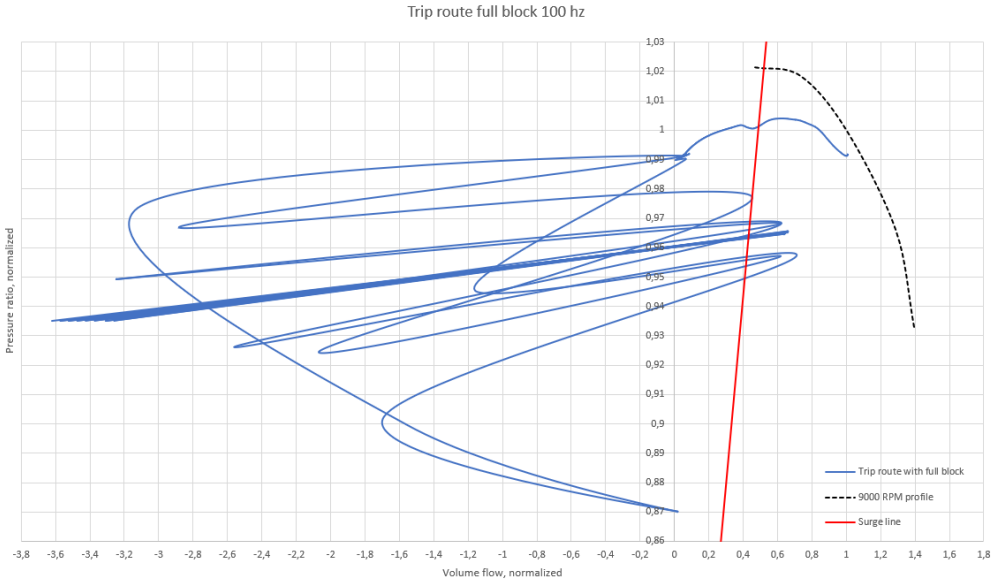

Figure 22: First 5 seconds of trip with blockage, 9000RPM, 100 hz

When the sampling frequency is increased it becomes apparent that a lot of information is lost at 10 hz. Firstly, an almost solid blue section is formed in the graph indicating full surge. It also becomes evident that the frequency of which the flow oscillates is well over 10 hz, as figure 22 shows that the flow oscillates at least ten times as fast as figure 21. Additionally, the full surge is evident close to half a second earlier with the increased sampling frequency. Back-flow happens only 4,7 seconds after trip, with full surge a tenth of a second later. This is despite the discharge valve still being about 1 % open, as a consequence of it operating by its data-sheet specifications. The 100 hz sampling frequency shows that the operating point of the compressor changes so rapidly that a 10 hz sampling rate paints a totally different, and inaccurate, picture of how the compressor behaves during trip.

The general trend of this simulation can be divided into three parts. In the first phase pressure builds up as volume flow decreases to close to zero, as expected when closing the discharge valve. Second phase is an initializing period where the compressor is surging with large changes in pressure

between each oscillation. This is then followed up by the long third phase where the compressor is in surge with a slowly decreasing pressure (referred to as "full surge").

However, the Hysys model does not manage to show what one would call expected behaviour of the compressor during surge, especially for the two last phases. There are some indications that the model is numerically unstable when trying to simulate surge. One example of unrealistic behaviour is the general trend of the compressor operating far to long in with negative flow compared to positive flow during surge. As the discharge valve at this point is fully closed, the compressor has no source it can draw the gas stream from. The model basically creates a gas stream from nothing. Furthermore the way the trip route in figure 22 behaves at its global minimum indicates a failing simulation as it is a somewhat improbable trip route.

Multiple attempts were made to stabilize the model while in surge, but none were effective. Especially closing of the discharge valve with the compressor running at full speed without trip resulted in the model failing to converge as early as at 30 % valve opening. Furthermore, when the compressor failed to converge it sometimes became fully bricked. It would not become stable when all parameters were restored to normal, showing impossible values for volume flow, temperature and compressor speed. The only solution found to this problem was to close the model without saving before opening it again, thus restoring it to how it was before running into surge.

4.5 Trip and blockage at 11000 RPM and 6000 RPM

To investigate whether or not the model managed a higher accuracy of its simulations under different operating conditions simulations were done at 11 000 RPM and 6000 RPM. Because of the low pressure of the compressor the affinity laws, or fan laws, could be used to calculate compressor curves for these two RPMs from the 9000RPM curve. Spreadsheet of this can be found in the appendix.

The results for the 11 000 RPM simulation, figure 23, are more or less the same as for the 9000 RPM simulation. It starts with a pressure build up as volume flow decreases by the closing of the discharge valve, which seems reasonable before the trip route goes into the same unrealistic behaviour as described for the 9000 RPM profile.

The suspicion of the model being numerically unstable early in the trip simulation seems to be just, as the simulation shuts down as the pressure solver fails to converge. This once again leads to the model being bricked. What was surprising was that the simulation failed to converge before the discharge valve had time to close, only six simulated seconds after trip, while the 9000 RPM trip simulation never did. This is not to be mistaken for a higher accuracy, as both simulations are well off their marks as soon as the compressor goes into surge.

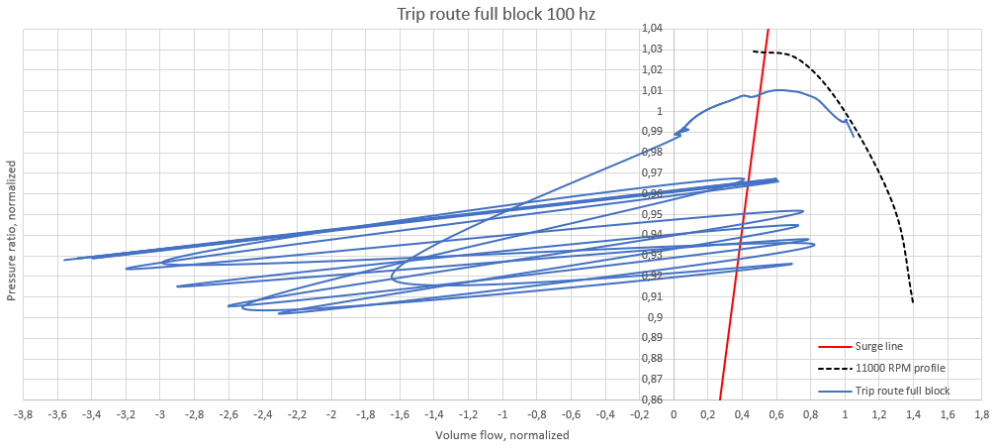

Figure 23: First 5 seconds of trip with blockage, 11000RPM, 100 hz

As for the 6000 RPM simulation the model failed to converge so early that there was no results to examine. Only 1,5 seconds after trip the simulation broke down, almost exactly as the operational point would have crossed the surge line. This once again resulted in a error message and bricking

of the model. If the model runs without trip, at any RPM, the discharge valve can only be closed to 31 % before the model fails to converge once again. Multiple attempts were done to resort this problem via the equation solver in Hysys but none were successful.

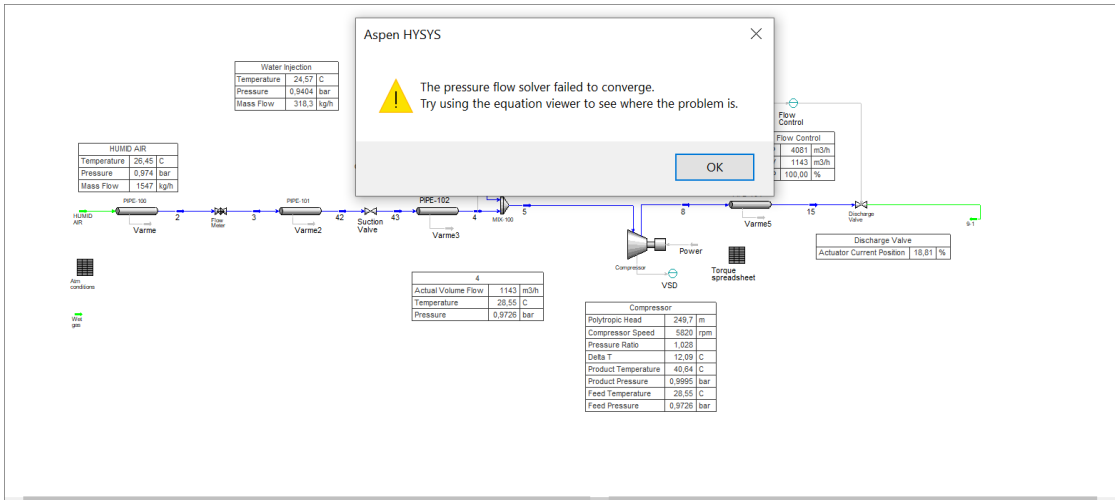

Figure 24: Hysys' "failed to converge"-error

There was a suspicion that the model failed to converge as a consequence of surge being inconsistent with the compressor curves. In an effort to guide the model in the correct direction a zero volume flow operational point was added to each of the compressor curves, as shown in figure 25. In this figure the operational point is at the point of failure to converge for the 9000 RPM simulation.

The zero volume flow operational points were combined with different head and efficiency values, altering the angle at which the straight line at the end of each curve would meet the y-axis. This had no effect, as the model failed to converge in the exact manner as before. It is worth noting that the model became unstable before reaching the end of the curve, shown by the operating point being to the right of the lowest volume flow point of the original curve. This indicates that the problem does not lie with the model being in need of a compressor curve down to zero volume flow.

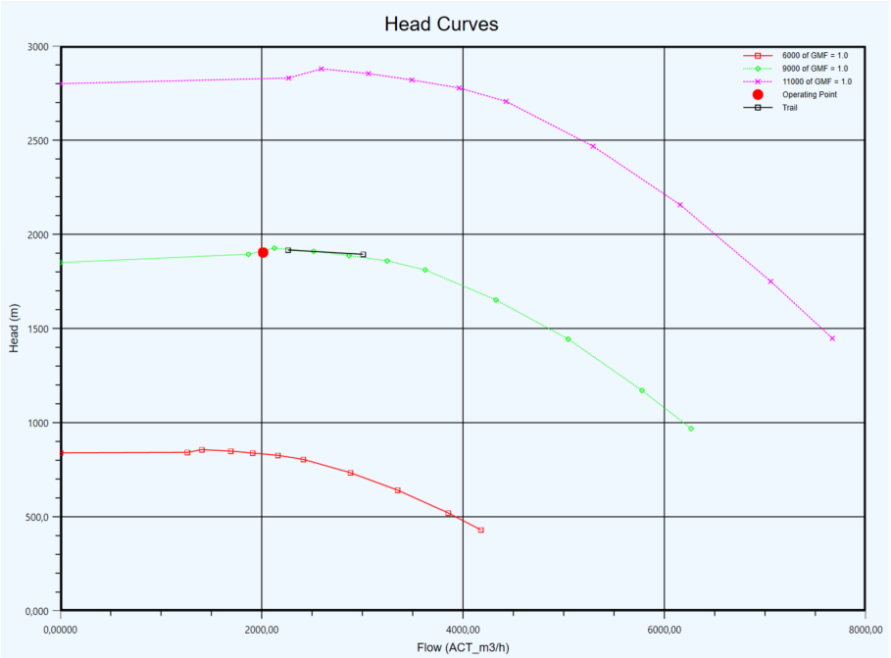

Figure 25: Compressor curves plotted in Hysys

For these simulations the model did not manage to simulate the expected behaviour of a compressor trip when forced into surge. The trip trajectory in the surge area is at best improbable and the model becomes numerically unstable.

4.6 Simulated trip on hydrogen gas

Dynamic process models such as the one used in this paper has the potential to estimate the performance and behaviour of a given compressor rig without actually building it. Testing facilities for compressors are also costly, especially if the fluid being processed is of a flammable nature. Hydrogen gas is just that, and because of its low ambient volumetric energy density is in need of being heavily compressed to become a practical energy carrier. As discussed earlier; compression of hydrogen gas is highly energy consuming, which in turn leads to increased installation cost due to the need of larger and more complex compression systems. Additionally, the possibility to simulate how an existing compressor rig behaves when the fluid is changed to hydrogen can be of value.

The mentioned problem with compressing hydrogen gas, its low molecular weight, results in a high head to pressure increase ratio. For all simulations the head curves for air were used, leading to a low pressure increase over the compressor. The simple trip, without ramping, is therefore of little or no interest and can be found in the appendix.

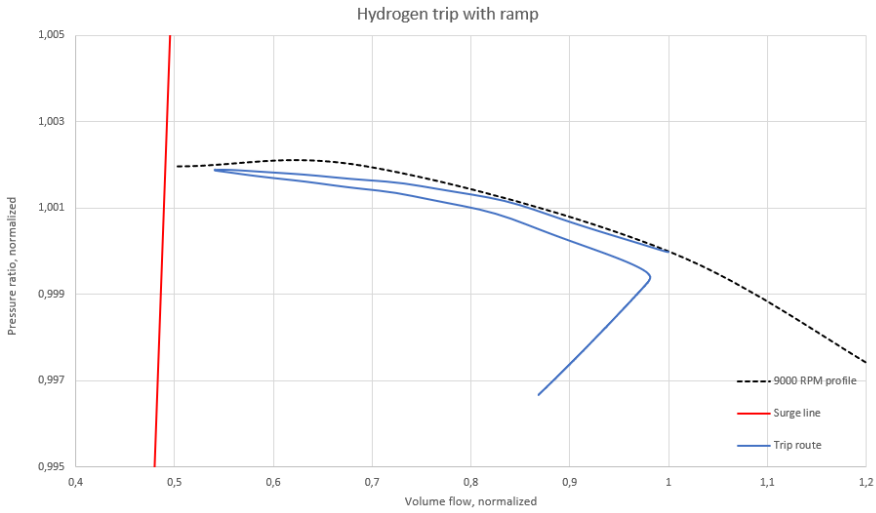

Figure 26: Simulated trip with ramping on hydrogen gas

As for the hydrogen trip with ramping the behaviour of the compressor was somewhat consistent with its behaviour on air. One clear difference between trip on the two fluids is that even though the discharge valve is programmed equally the trip route is closer to the 9000 RPM profile for hydrogen. A reason to this is that because of the low mass flow to volume flow ratio of hydrogen gas it has a much lower breaking effect on the compressor impeller after trip. This was also evident by the compressor barely losing RPM during the whole ramping process. When simulating with hydrogen

the compressor had a speed of 8863 RPM when the ramping of the discharge valve was completed 6,8 seconds after trip. The speed of the compressor was down to 7613 RPM at the same point when running the model on air. For hydrogen the compressor is close to producing the same pressure increase in the fluid throughout the whole simulation as evident by the scale of the y-axis in figure 26.

The simulations of trip with ramping were promising as they showed the compressor behaving as expected. This can not be said for the trip simulations for hydrogen with full blockage of the discharge pipe.

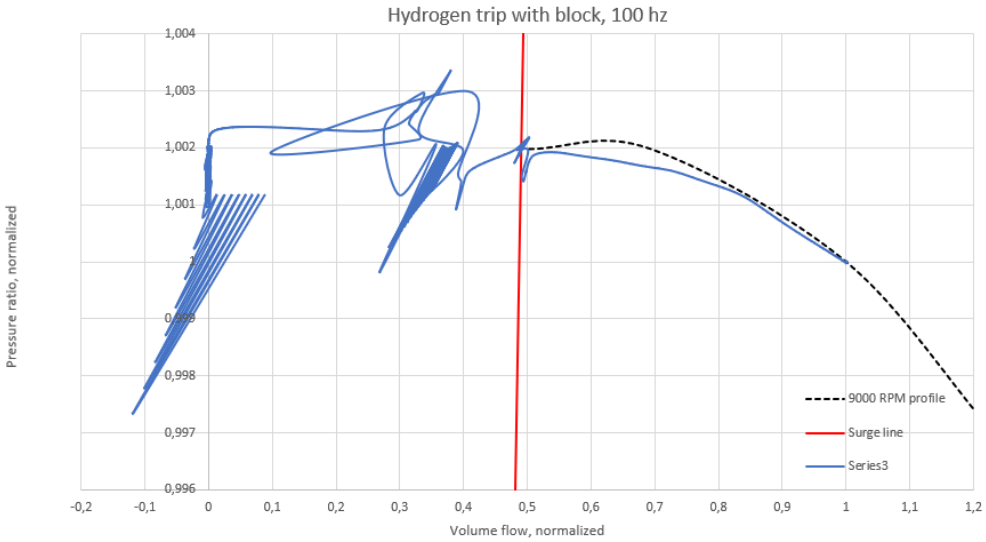

Figure 27: Simulated trip with full block on hydrogen gas

As with the simulations with blockage on air the model manages to simulate the trip until the compressor crosses the surge line. The highly erratic trip route once again indicates a numerically unstable model. Additionally, when the discharge valve reaches zero percent opening the volume flow remains positive for five seconds, and as the trip route hits the y-axis the compressor still has a pressure increase over it. For this simulation the balance between positive and negative volume flow seems more reasonable when the compressor is in full surge, compared to the simulations on air. However, this does not mean that the model is accurate. For both hydrogen gas simulations the head curves for air was used, resulting in a small pressure increase over the compressor as discussed in the "Air to hydrogen gas conversion procedure"-chapter.

The model managed to simulate the trip trajectory for the trip-scenario with ramping. While doing

so, the simulation highlighted the reduced pressure increase for hydrogen gas compared to air. For the simulations with blockage of the compressor discharge, the results were similar to the simulations for air with the model showing severe instabilities.

5 Conclusion

A conversion procedure for centrifugal compressors has been established, converting air to hydrogen performance. This procedure shows the reduction in pressure ratio for a compressor when changing fluid to hydrogen gas, as a result of lower molecular weight of the fluid. A procedure for Reynolds correction is also added, as the best estimate to changes in efficiency for the compressor when changing fluid.

The NTNU wet gas compressor model in Hysys dynamics has been tuned to the compressor rig's current layout while running on air. It is important to note that the ambient conditions play a big role in performance of the compressor. The model was tuned based on one set of ambient conditions, and compared to the compressor running on a slightly different set of ambient conditions. Comparing the results from the reference tests, both steady and transient, showed satisfying levels of accuracy when accounting for the change in ambient conditions. This accuracy is dependent on the compressor not running into surge.

As for dynamic simulation of the compressor when running into surge, there were not much knowledge to be gained except from confirming that Hysys Dynamics is not able to execute an accurate simulation for a compressor in this state. The model became numerically unstable, and in several instances would not manage to recover even when reverting to the input variables of for example best efficiency point, which it had managed to simulate before. Efforts were made to find research regarding simulation of surge for centrifugal compressors without much luck. Most papers found on the subject focuses on either near surge operation or surge initiation.

6 Future work

There were multiple interesting areas that emerged during the work with this thesis. Firstly, developing a dynamic model that is numerically stable for a compressor in surge could be highly beneficial for the industry. This is of course a tall order. It would also be interesting to examine whether or not Hysys dynamics manages to simulate a trip scenario for hydrogen gas with a higher pressure delta than in this thesis, and if possible to verify the simulation.

Another area in need of further work is the exploration of forward-facing impeller vanes for hydrogen compressors. As mentioned earlier the reasoning behind radial and backward-facing impeller vanes being the industry standard is to avoid chocking at impeller exit. With hydrogen's high sonic velocity there is a possibility of increased performance for centrifugal hydrogen compressors utilizing this. Higher pressure ratio at lower rotational speed, as a result of the vane angle, seem like a promising prospect with regards to friction and bearing losses and general durability of the compressor. This would require a rather high level of CFD (Computational fluid dynamics) competence.

The differences between a trip scenario for an air- and a hydrogen compressor could also be more extensively studied as the as the model in this thesis became numerically unstable when the compressor entered surge. Here, the low breaking effect hydrogen gas has on the impeller is especially interesting, as it would result in a lower drop-off in pressure ratio per time after trip. The effect the light molecular weight of hydrogen gas has on a high pressure compressor during trip would be of special interest.

Bibliography

[1] Çengel, Y. A., . B. M. A. 1994. *Thermodynamics: An engineering approach*. McGraw-Hill.

[2] Dixon, S. L. & Hall, C. A. 2014. *Fluid Mechanics and Thermodynamics of Turbomachinery*. Butterworth-Heinemann.

[3] Hannu Jääskeläinen, M. K. K. 2017. Dieselnet website. https://www.dieselnet.com/tech/air_turbocharger.php. Accessed: 2019-11-01.

[4] Gisle B. Tveit, Lars E. Bakken, T. B. 2004. Compressor transient behaviour. *ASME Turbo Expo 2004: Power for Land, Sea, and Air*, 7, 813–821. doi:https://doi.org/10.1115/GT2004-53700.

[5] McMillan, G. K. 2010. *Centrifugal and Axial Compressor Control*. Momentum Press.

[6] L. Bakken, E. Lunde, M. L. 2016. Power dip impact on compressor system stability. *Proceedings of ASME Turbo Expo 2016: Turbomachinery Technical Conference and Exposition*, 9.

[7] Ø. Hundseid, L. B. 2015. Integrated wet gas compressor facility. *ASME Turbo Expo*, 9. doi:https://doi.org/10.1115/GT2015-43004.

[8] National institute of standards and technology. 2020. Download for mini-REFPROP: https://trc.nist.gov/refprop/MINIREF/MINIREF.HTM. Accessed: 2020-02-13.

[9] R.A Strub, L. Boniani, C. J. B. M. V. C. S. L. C. B. B. C. J. K. H. S. M. A. S. 1987. Influence of the reynolds number on the performance of centrifugal compressors. *Journal of Turbomachinery*, 109, 541–544.

[10] Savić, V., Knežević, D., Lovrec, D., Mitar, J., & Karanovic, V. 2009. Determination of pressure losses in hydraulic pipeline systems by considering temperature and pressure. *Strojniski Vestnik*, 55, 237–243.

[11] Abdelwahab Aroussi, F. B. 2012. *Proceedings of the 3rd Gas Processing Symposium*. Elsevier.

[12] Heshmat, D. H. Mohawk industries inc. presentation for us doe. E-mail exhange with Mohawk Industries.

[13] M.Bakken. Transient analysis of wet gas compressor systems. *Doctoral Theses at NTNU, 2019:159, ISBN: 978-82-326-3917-5*.

A Appendix

A.1 Calculated compressor curves for 6000 RPM and 11000 RPM

9000rpm profile					
volume flow, Q (m^3/s)	0,557231	0,871237	1,189247	1,532613	1,659872
pressure ratio	1,23354	1,230063	1,207831	1,166667	1,126737

Calculated 11000 rpm profile					
volume flow, Q (m^3/s)	0,68106	1,064846	1,453524	1,873194	2,028733
pressure ratio	1,348869	1,343674	1,310463	1,248971	1,189324

Calculated 6000 rpm profile					
volume flow, Q (m^3/s)	0,371487	0,580825	0,792831	1,021742	1,106582
pressure ratio	1,103796	1,10225	1,092369	1,074074	1,056328

Affinity laws:

Q1 / Q2 = (n1 / n2)

Hp1 / Hp2 = (n1 / n2)^2

Note:
Formula uses head (Hp), profiles uses pressure ratio

Calculated 11000 rpm profile normalized					
volume flow, Q	0,468558	0,732596	1	1,288726	1,395734
pressure ratio	1,029307	1,025343	1	0,953076	0,90756

Calculated 6000 rpm profile normalized					
volume flow, Q	0,468558	0,732596	1	1,288726	1,395734
pressure ratio	1,01046	1,009046	1	0,983252	0,967006

A.2 Simulated simple compressor trip with Hydrogen

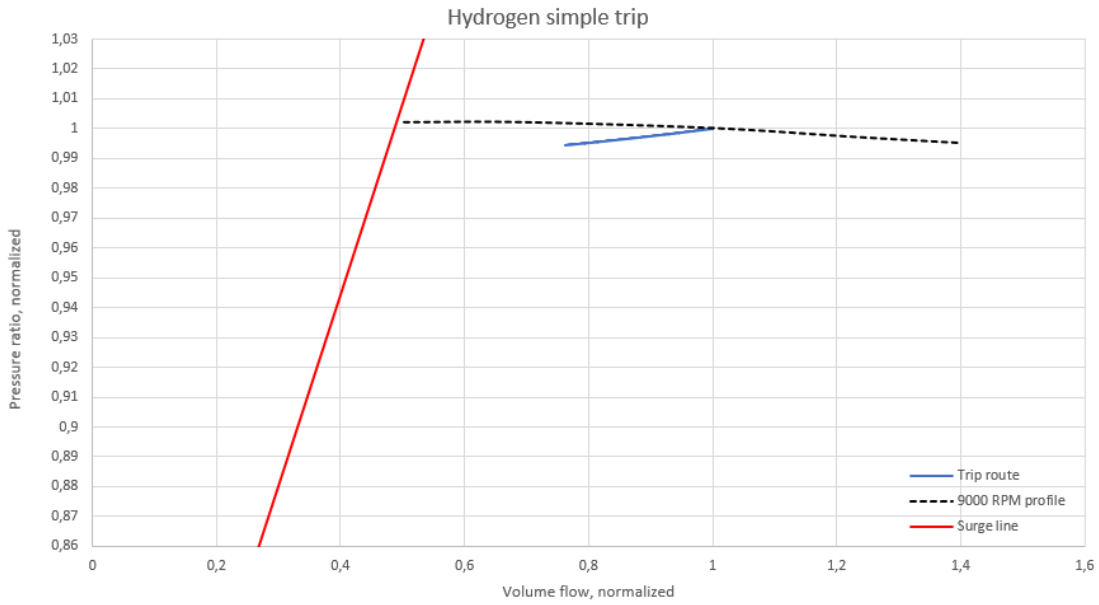

A.3 Air to hydrogen gas conversion and reference tests values

Conversion to hydrogen gas, REFPROP						
Valve opening (%)	30	42	54	75	100	
cp/cv (air)	1,409	1,409	1,410	1,409	1,408	from hysys
Z (air)	1,000	1,000	1,000	1,000	1,000	from hysys
p2/p1 (air)	1,236	1,231	1,210	1,165	1,127	from experiment
T1(air, K)	299,995	300,320	299,870	300,520	300,458	from experiment
polytropic efficiency	0,686	0,726	0,770	0,721	0,642	from hysys
polytropic exponent	1,733	1,666	1,607	1,674	1,823	
Polytropic head (j/kg)	18310,638	17985,611	16506,503	13252,832	10365,002	calculated
cp/cv (hydrogen)	1,405	1,405	1,405	1,405	1,405	from refprop
polytropic exponent	1,725	1,658	1,598	1,667	1,815	calculated
Z (hydrogen)	1,001	1,001	1,001	1,001	1,001	from refprop
p2/p1 (hydrogen)	**1,015**	**1,015**	**1,013**	**1,011**	**1,008**	calculated
T1 (hydrogen, K)	299,995	300,320	299,870	300,520	300,458	same as air
T2 (hydrogen, K)	301,860	302,050	301,367	301,805	301,586	calculated

ref.test1					
Valve opening (%)	30	42	54	75	100
Dp_orifice	10,210	21,380	40,900	65,940	85,050
PT3.3	994,300	993,070	992,450	989,610	988,080
TT5.1	25,610	25,960	25,630	26,260	26,390
P_inlet	983,660	971,000	950,260	921,470	899,860
T_inlet	26,845	27,170	26,720	27,370	27,308
P_outlet	1215,400	1195,000	1150,000	1073,670	1014,170
T_outlet	50,800	49,350	45,890	43,925	41,830
Rel hum	26,160	28,050	32,980	34,720	35,790
Torque	20,460	25,930	30,490	31,940	31,010
mass flow	0,649	0,935	1,284	1,613	1,817
volume flow	0,568	0,830	1,163	1,509	1,742
pressure ratio	1,236	1,231	1,210	1,165	1,127
Normalized Q BEP	0,488	0,713	1,000	1,298	1,497

ref.test2					
Valve opening (%)	30	42	54	75	100
Dp_orifice	9,625	23,150	41,900	66,900	83,950
PT3.3	976,800	975,300	974,000	971,750	970,150
TT5.1	26,320	26,430	26,450	26,300	26,050
P_inlet	966,000	953,000	932,250	904,500	883,125
T_inlet	27,600	27,660	27,580	27,340	26,970
P_outlet	1191,600	1172,250	1126,000	1055,250	995,050
T_outlet	53,800	51,180	48,100	44,550	41,900
Rel hum	27,400	31,100	36,300	39,900	41,750
Torque	20,300	26,300	30,500	32,000	31,100
mass flow	0,624	0,962	1,285	1,607	1,702
volume flow	0,557	0,871	1,189	1,533	1,660
pressure ratio	1,234	1,230	1,208	1,167	1,127
Normalized Q BEP	0,469	0,733	1,000	1,289	1,396

A.4 The Moody Diagram

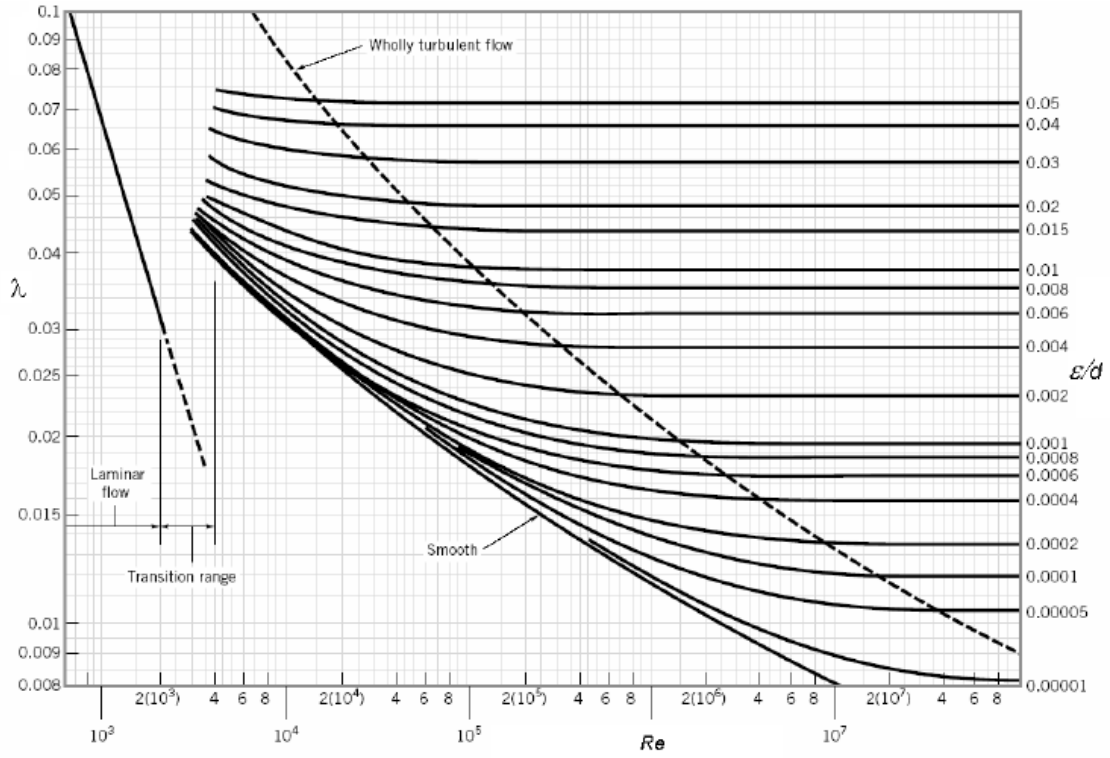

[10]

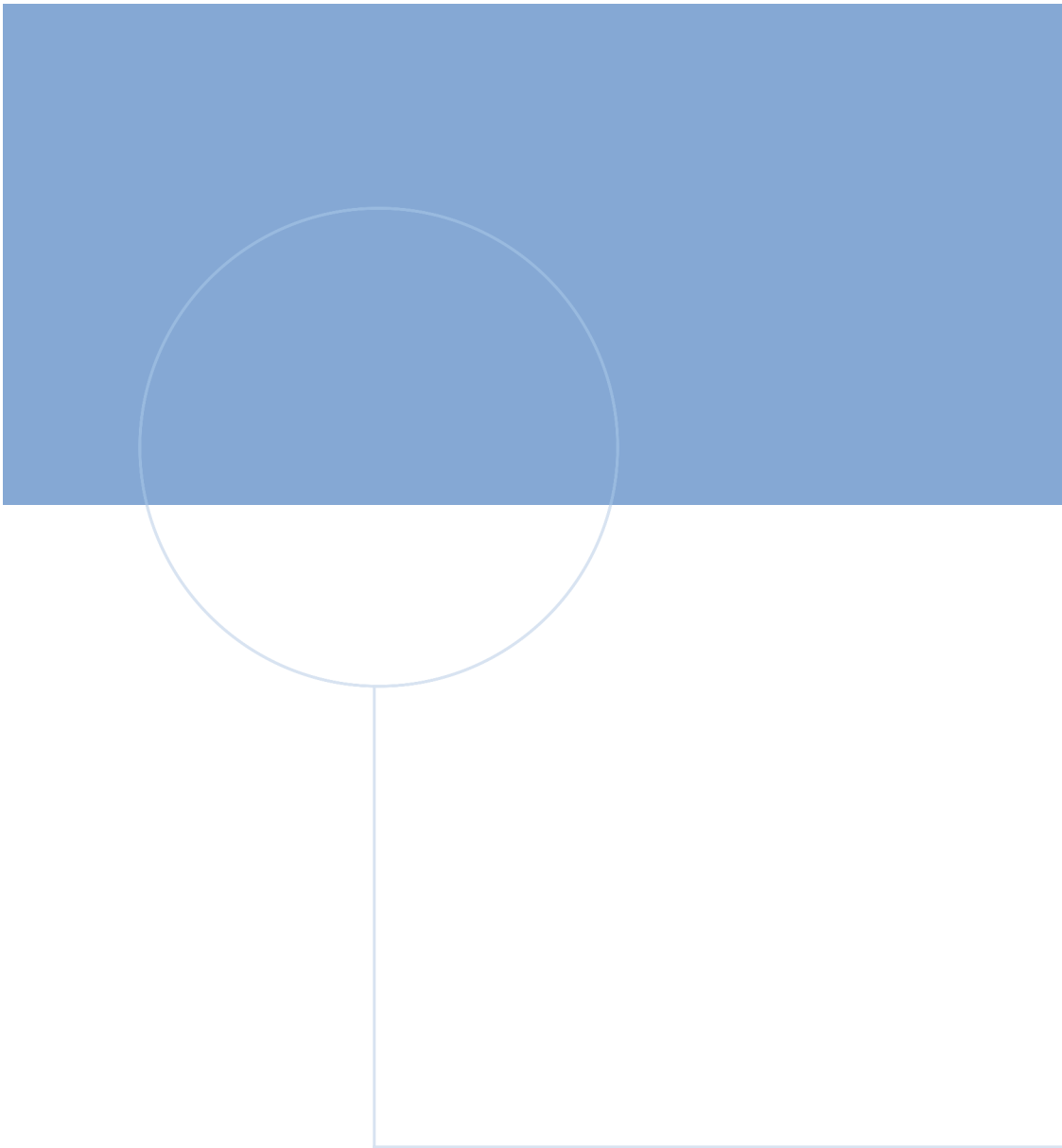

NTNU

Norwegian University of
Science and Technology